MER-0003-FM-9234-501

BRIDGE FATIGUE LIFE INDICATING SYSTEM

D. Thomson
G. Samavedam
Foster-Miller, Inc.
350 Second Avenue
Waltham, MA 02154-1196

September 1991

Final Report
Contract No. DAAK70-91-C-0003

Prepared for:

Belvoir RD&E Center
Ft. Belvoir, VA 22060-5606

MER-0003-FM-9234-501

BRIDGE FATIGUE LIFE INDICATING SYSTEM

D. Thomson
G. Samuedam
Foster-Miller, Inc.
350 Second Avenue
Waltham, MA 02154-1196

September 1991

Final Report
Contract No. DAAK70-91-C-0003

Prepared for:

Belvoir RD&E Center
Ft. Belvoir, VA 22060-5606

UNCLASSIFIED
SECURITY CLASSIFICATION OF THIS PAGE

REPORT DOCUMENTATION PAGE

1a. REPORT SECURITY CLASSIFICATION Unclassified	1b. RESTRICTIVE MARKINGS
2a. SECURITY CLASSIFICATION AUTHORITY Unclassified	3. DISTRIBUTION/AVAILABILITY OF REPORT
2b. DECLASSIFICATION/DOWNGRADING SCHEDULE N/A	
4. PERFORMING ORGANIZATION REPORT NUMBER(S) MER-0003-FM-9234-501	5. MONITORING ORGANIZATION REPORT NUMBER(S)
6a. NAME OF PERFORMING ORGANIZATION Foster-Miller, Inc.	6b. OFFICE SYMBOL (If applicable)
	7a. NAME OF MONITORING ORGANIZATION DCMAO
6c. ADDRESS (City, State, and ZIP Code) 350 Second Avenue Waltham, MA 02154-1196	7b. ADDRESS (City, State, and ZIP Code) 495 Summer Street Boston, MA 02210-2184
8a. NAME OF FUNDING/SPONSORING ORGANIZATION Belvoir RD&E Center	8b. OFFICE SYMBOL (If applicable) STRBE-JBC
	9. PROCUREMENT INSTRUCTION IDENTIFICATION NUMBER DAAK70-91-C-0003
8c. ADDRESS (City, State, and ZipCode) Fort Belvoir, VA 22060	10. SOURCE OF FUNDING NUMBERS

PROGRAM ELEMENT NO.	PROJECT NO.	TASK NO.	WORK UNIT ACCESSION NO.
N/A	MER-9234	A003	N/A

11. TITLE (Include Security Classification)
Bridge Fatigue Indicating System

12. PERSONAL AUTHOR(S)
D. Thomson, G. Samavedam

13a. TYPE OF REPORT	13b. TIME COVERED	14. DATE OF REPORT (Year, Month, Day)	15. PAGE COUNT
Final	FROM 11/90 TO 9/91	1991 September 6	76

16. SUPPLEMENTARY NOTATION

17. COSATI CODES			18. SUBJECT TERMS (Continue on reverse if necessary and identify by block number)
FIELD	GROUP	SUB-GROUP	
15	07		Fatigue, Crack Growth, Military Bridges, Crack Measurement
14	03		

19. ABSTRACT (Continue on reverse if necessary and identify by block number)

The Twin Coupon FLI system which is suitable for use on mobile Army bridges has been developed, enhanced, and field tested in this program. The device utilizes two precracked aluminum coupons attached directly to the bridge. By measuring the crack lengths in the coupons, and knowing the initial crack lengths, the stress and cycles applied to the bridge can be directly calculated.

A previous program conducted extensive laboratory tests to define the crack growth rates and develop a computer program to calculate the loading history. This program demonstrated the system in field crossing tests of the Armored Vehicle Launched Bridge (AVLB) at Aberdeen Proving Grounds.

Several system enhancements were concurrently developed in the laboratory. Numerous tests demonstrated a bonded attachment method for the coupons which eliminates the bridge damage which could result from the original bolted attachment method. Several remote crack measurement systems were evaluated and an accurate method, which would permit complete sealing of the coupons, was demonstrated. The potential for reduction of the coupon size was also shown in the laboratory.

This report presents field data and correlations from the vehicle crossing tests on the AVLB during the period of Jaunary to April 1991 a total of four two-coupon sets were applied to the two AVLBS for 2,000 crossing tests at Aberdeen Proving Grounds. The test results provided adequate proof of the Twin Coupon Concept.

20. DISTRIBUTION/AVAILABILITY OF ABSTRACT	21. ABSTRACT SECURITY CLASSIFICATION
___ UNCLASSIFIED/UNLIMITED x SAME AS REPORT ___ DTIC USERS	Unclassified

22a. NAME OF RESPONSIBLE INDIVIDUAL	22b. TELEPHONE (Include Area Code)	22c. OFFICE SYMBOL
D. Thomson	(617) 890-3200	N/A

TABLE OF CONTENTS

TABLE OF CONTENTS (Continued)

Section **Page**

TABLE OF CONTENTS (Continued)

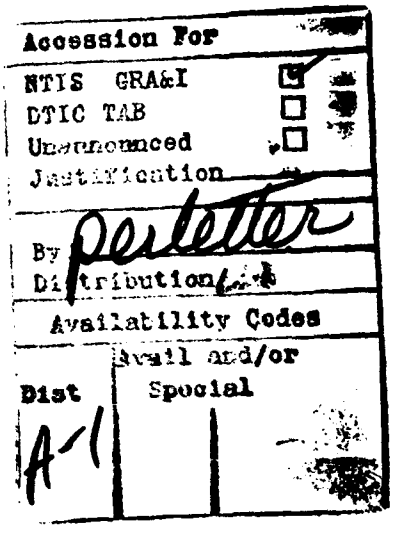

LIST OF ILLUSTRATIONS

Figure **Page**

LIST OF ILLUSTRATIONS (Continued)

Figure **Page**

LIST OF TABLES

1. PROGRAM SUMMARY

This program involved the continued development and field proof-of-concept of the Twin Coupon Fatigue Life Indicator (FLI) system. The tasks are defined in the contract DAAK70-91-C-0003. The Technical Program Officer at Ft. Belvoir, VA is Brian Hornbeck. The work performed in each task is summarized below and described in detail in later sections.

Task 1 - Identify Stress and Fatigue Critical Locations

The Armored Vehicle Launched Bridge (AVLB) has been selected for field proof-of-concept tests. Static and crossing test strain data and test results for this bridge were reviewed to define the stresses and critical locations. Static and crossing tests were monitored, bridge geometry was measured and additional strain gauges were applied to evaluate the proposed FLI attachment location.

Task 2 - Develop Coupon Attachment Method

Numerous adhesives were tested in the laboratory and both bolted and bonded attachment methods were demonstrated. The bolted attachment technique was fully developed at the time of field testing of the AVLB by the Army and thus was used for the field validation of the twin coupon concept.

Task 3 - Develop Field Crack Length Measurement System

Three potential systems were evaluated to develop a remote crack measurement system. AC Potential Drop (ACPD) was found to be unacceptable. Ladder gauges were found to be acceptable with several significant limitations. The Krak Gage system demonstrated superior performance and is recommended for field development.

Task 4 - Optimize Coupon Size

Options to permit coupon size reduction (bonded attachment and improved crack measurement) were considered. A preliminary assembly test was conducted with coupons of significantly reduced size to demonstrate that further coupon size reduction is possible for future applications.

Task 5 - Field Installation of FLI

A total of four of the FLI sets were fabricated and installed to two AVLBs for crossing tests at Aberdeen Proving Grounds (APG), MD. One set was designed for a life of 2000 crossings and another set was designed for the standard life of 10,000 crossings.

Task 6 - Test Support

Test support was provided during the crossing tests at APG and the static tests at Ft. Belvoir, VA. Test support included fatigue life indicator system installation, test monitoring, data acquisition and real-time data analysis.

2. INTRODUCTION

2.1 Military Bridge Design

Military bridges are designed to carry substantial loads, yet must be easily moved and quickly erected in tactical field situations. This requires a modular design utilizing high strength-to-weight ratio materials. To further enhance portability, bridge weight is minimized by sacrificing ultimate and fatigue strength in a tradeoff with useful life. The final result is a lightweight bridge with a useful, but limited, life.

These bridges must be removed from service before their useful life is exceeded. This poses a serious problem, as individual bridges are used at various locations over different spans with generally undefined traffic patterns. At present, there is no accurate way to determine when a given bridge is approaching its useful life and needs to be removed from service. Therefore, there is a need for a technique for measuring the actual service that the bridge has seen and for relating that service to the predicted fatigue life.

Bridge fatigue damage requires an appropriate quantitative evaluation. The fatigue damage can be seen in the form of fatigue cracks emanating from rivet holes, hinges, weldments and other fatigue critical locations. Hidden cracks such as under rivet heads may also exist, which may need NDI. Although crack size can be used as a measure of fatigue life consumed, their inspection in field service may not be practical. However, knowledge of maximum permissible crack size in the bridge should be established through fracture mechanics and damage tolerance analysis. This will determine the maximum possible fatigue life for the bridge structure before a major catostrophic fracture failure will occur. With this information, a fatigue device can be designed to monitor the percent of total fatigue life consumed at any given instant in service.

2.2 Twin Coupon Concept Basis

The Twin Coupon method works on the well-established principle of fracture mechanics. Figure 1 shows the crack growth rate versus the stress intensity factor at the crack tip. Region I represents a combination of crack initiation and microcrack development period. Region II represents the well-known Paris region in which the crack growth law is well-defined and *linear*. The Twin Coupons are designed to operate essentially in the Region II. This is accomplished by precracking the coupons and removing the uncertainty with crack initiation in Region I.

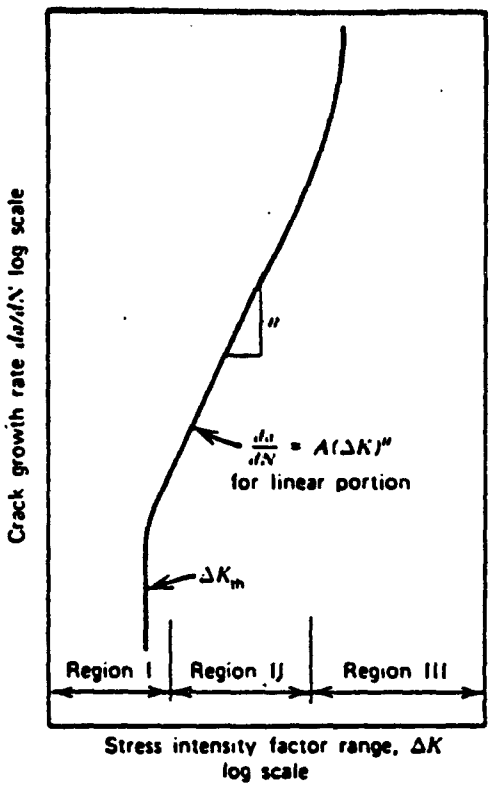

Figure 1. Schematic Sigmoidal Behavior of Fatigue Crack Growth versus ΔK

The concept utilizes precracked fatigue coupons, rigidly fastened to any bridge structural member under tension. The attachment makes the coupons experience the same number of cycles and proportional stress levels as the structural member. With rational coupon design, using fracture mechanics theory for crack propogation, the crack length at any instant can be used as a measure of the consumed fatigue life of the bridge structural element under evaluation. (It is not necessary to mount the coupon on the particular bridge element of concern). Using twin coupons of different materials, mounted at similar locations, so that they experience the same applied stress, and measuring both crack lengths from time to time, the stress histograms (stress versus cycles) can be deduced. This is the significant advantage over single coupon designs. Since two coupons of different materials are used, both unknowns (stress and cycles) can be determined by measuring the two crack lengths. In single coupons, one of these quantities must be known in order to determine the other. The stress at the coupon location can then be used to determine the stress of other fatigue critical locations.

To show how the histograms can be deduced using the concept let us assume that we have two coupons with different crack lengths and of different materials. The two coupons will be

respectively represented by suffixes 1 and 2. The equation for crack propagation in coupon No. 1 is:

$$\frac{da_1}{dN} = C_1 \Delta K_1^{\ n_1} \tag{1}$$

For simplicity, we use the expression for K as that of the infinite plate. The finite plate expressions do not pose special problems.

$$\Delta K_1 = \Delta_1 \sigma_1 \sqrt{\pi a_1} \tag{2}$$

For coupon No. 2 the equation is:

$$\frac{da_2}{dN} = C_2 \Delta K_2^{\ n_2} \tag{3}$$

$$\Delta K_2 = \Delta \sigma_2 \sqrt{\pi a_2} \tag{4}$$

The two coupons will have equal strains, and thus for coupon materials with the same moduli, we have $\Delta\sigma_1 = \Delta\sigma_2$.

The number of cycles (N) is defined by integrating Equation 1.

$$N = \frac{a^{1-n/2} - a_i^{1-n/2}}{c\Delta\sigma^{n}\pi^{n/2}(1-n/2)} \tag{5}$$

Since the stress cycle ($\Delta\sigma$) and the number of cycles (N) is the same for both coupons, $\Delta\sigma$ is defined from Equation 5 as:

$$\Delta\sigma = \left[\frac{c_2 \pi^{\frac{n_2}{2}} \left(1 - \frac{n_2}{2}\right) \left(a_1^{1 - \frac{n_1}{2}} - a_{1_i}^{1 - \frac{n_1}{2}} \right)}{c_1 \pi^{\frac{n_1}{2}} \left(1 - \frac{n_1}{2}\right) \left(a_2^{1 - \frac{n_2}{2}} - a_{2_i}^{1 - \frac{n_2}{2}} \right)} \right]^{\frac{1}{n_1 - n_2}} \quad (6)$$

Using this equation, the stress cycle, and consequently the number of cycles, may be calculated. This calculated stress cycle is a weighted average of all of the vehicle crossings (N). This loading history may then be used to calculate the fatigue life consumed.

2.3 Previous Work

The Fatigue Life Indicator (FLI) system was developed and demonstrated in numerous laboratory tests. This system included a computer program which was written to deduce the stress histograms based solely on the measurement of the coupon crack lengths. This indicator demonstrated the potential to provide service life information not currently available for military bridges.

A method was developed for fabrication of the coupons which included precracking of the coupons at a low stress level of 15 Ksi to avoid crack retardation at the operational levels of the AVLB. Optical crack measurement was found to have sufficient resolution under laboratory conditions. Tests were conducted to define the Paris Law constants (c,n) for the two coupon materials. A linear fit was made to the 2024-T3 data while a bi-linear fit through a transition point was required for the 6061-T6 data.

A BASIC computer program was written to deduce the loading history based on the two crack lengths. The program uses the initial and final crack lengths to calculate the stress cycle using Equation 6. For this first calculation, the below transition constants for 6061-T6 are used. A check is then made to determine if transition has been exceeded for the stress level. If transition is exceeded, the stress level above transition is calculated using Equation 6 and the above transition constants for 6061-T6. The two calculated stress levels are compared and an iteration process followed until these stress levels are equal. The total number of cycles at this stress level is then calculated using Equation 5. The stress cycle and number of cycles are the output of this program.

A test assembly was designed with the two FLI coupons attached to a representative bridge structure using a bolted attachment as shown in Figure 2. Tests were first conducted to define the Paris Crack Law constants C and n. Four assemblies were then tested to verify the operation of the system in the laboratory. As shown in Table 1, the agreement of the applied test loads and cycles with the computer prediction is very good. The one problem that did surface in Assemblies H and I was that precracking at a higher stress level can cause retardation of crack growth. This problem was corrected for Assemblies J and K. Based on the data from these tests, the system was considered functional in the laboratory with need of field proof-of-concept.

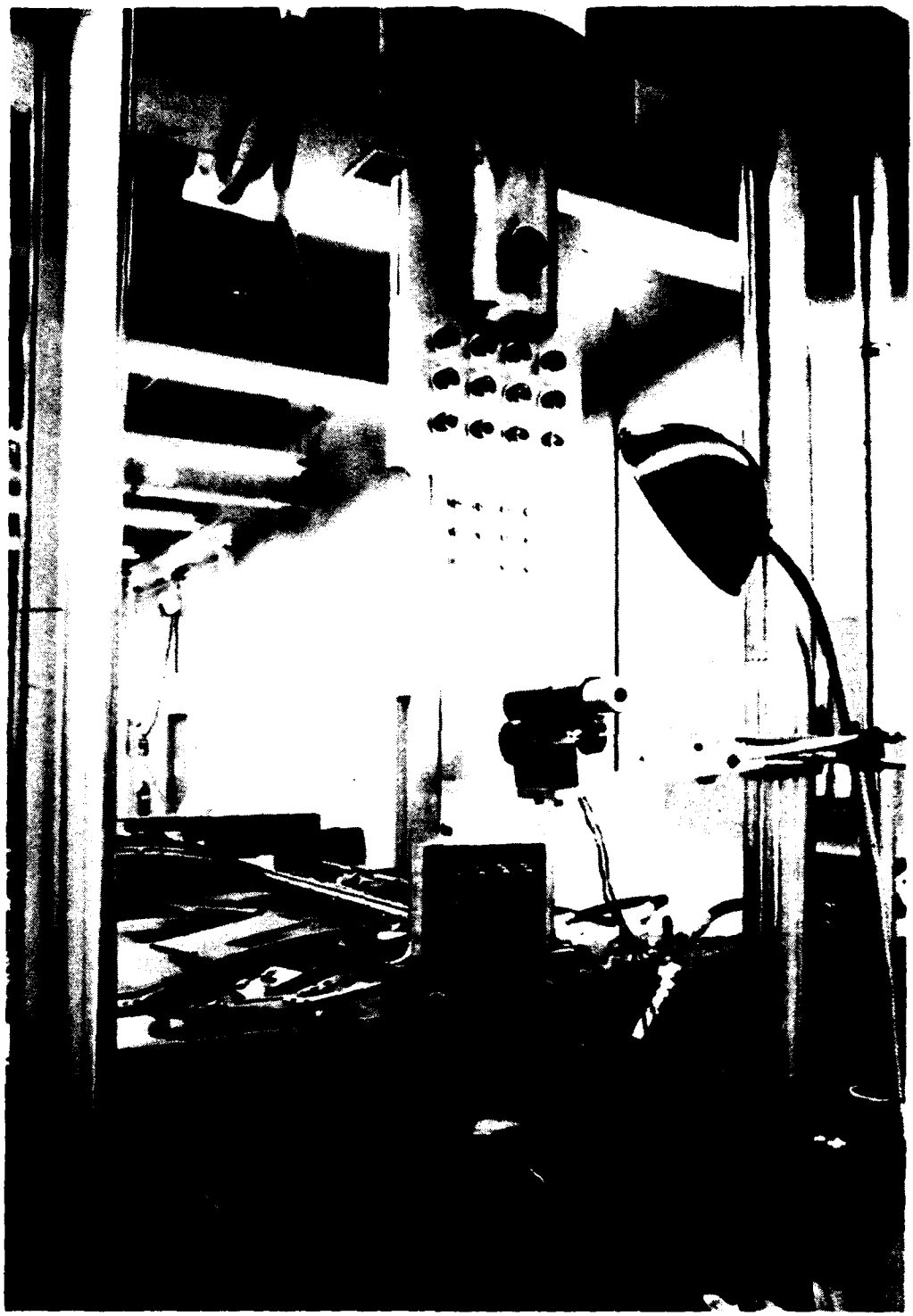

Figure 2. Test Assembly with Two FLI Coupons Attached to a Representative Bridge

Table 1. Test Results versus Predictions

Assembly	Test Results		Predictions	
	Cycles	Stress (Ksi)	Cycles	Stress (Ksi)
H	0	20.0		
	2,000	20.0		
	4,000	20.0	400	37.1
	6,000	20.0	900	31.9
	0	25.0		
	500	25.0	500	29.5
	1,000	25.0	1,200	26.3
	1,500	25.0	2,300	24.3
	2,000	25.0	2,700	24.8
	2,500	25.0	3,500	24.7
	3,000	25.0	3,800	25.5
I	0	20.0		
	2,000	20.0		
	4,000	20.0	300	38.0
	6,000	20.0	1,300	29.2
	0	25.0		
	1,000	25.0	1,200	23.6
	1,500	25.0	1,700	23.7
	2,000	25.0	2,400	23.1
	2,500	25.0	3,100	23.2
	3,000	25.0	4,000	22.6
	3,500	25.0	5,900	21.5
	4,000	25.0	6,500	21.9
	4,500	25.0	7,300	22.5
J	0	17.0		
	2,000	17.0	1,500	18.4
	4,000	17.0	3,300	17.8
	5,200	17.0	4,300	17.9
	6,000	17.0	4,700	18.1
	7,000	17.0	5,700	17.9
	8,000	17.0	6,800	17.7
	9,065	17.0	7,900	17.6
	10,000	17.0	8,900	17.4
	11,000	17.0	9,800	17.5
	12,000	17.0	11,000	17.3
	13,000	17.0	12,000	17.3
	14,000	17.0	13,100	17.3
	15,000	17.0	14,400	17.4
K	0	20.0		
	2,000	20.0	2,200	20.4
	4,000	20.0	4,000	20.0
	6,000	20.0	7,000	18.9

3. IDENTIFY STRESS AND FATIGUE CRITICAL LOCATIONS

3.1 Armored Vehicle Launched Bridge

The Armored Vehicle Launched Bridge (AVLB), shown in Figure 3, is a scissors launched mobile army bridge rated for Class 60 crossings at a span of 60 ft. The bridge superstructure has two treadways interconnected by cross bracings. Each of the treadways is of tapered construction comprised of two identical girders connected through a structural hinge. Each girder is of riveted plate/girder construction.

The deck is comprised of a number of extrusions that span transverse to the bridge length. These extrusions are bolted to the top flange of the tapered plate girder. Tapered vertical plates, forming the girder webs, are riveted to the bottom and top flanges to form the plate girder. The webs of each girder are connected by a number of diagonal and horizontal members to provide cross sectional rigidity.

When a vehicle traverses the bridge, its load is transferred from the deck to the plate girder and finally to the banks. The mechanisms of load transfer in the treadway are through flexural bearing, direct shear and torsional shear stresses. The predominant load transfer at the treadway center is by flexure and at the ends by shear. The flexure causes tensile stresses in the treadway's bottom chord.

The bridge is fabricated primarily from 2014-T6 aluminum which comprises the girders and cross members. Steel construction is used for the girders in the first 12 ft of the primary bridge ramp, as shown in Figure 3. This is required as the maximum shear stresses will occur in this section. The dead weight of the bridge is 29,300 lb.

The test programs have been conducted to qualify the bridge for Class 70 crossings at a span of 53 ft.

3.2 Static Analysis

A static analysis of the AVLB has been conducted using beam theory to define the applied stresses for the Class 70 crossings. A tank footprint of 14.8 ft was assumed as this was the footprint used for load application during static testing at Ft. Belvoir. For a configuration of both

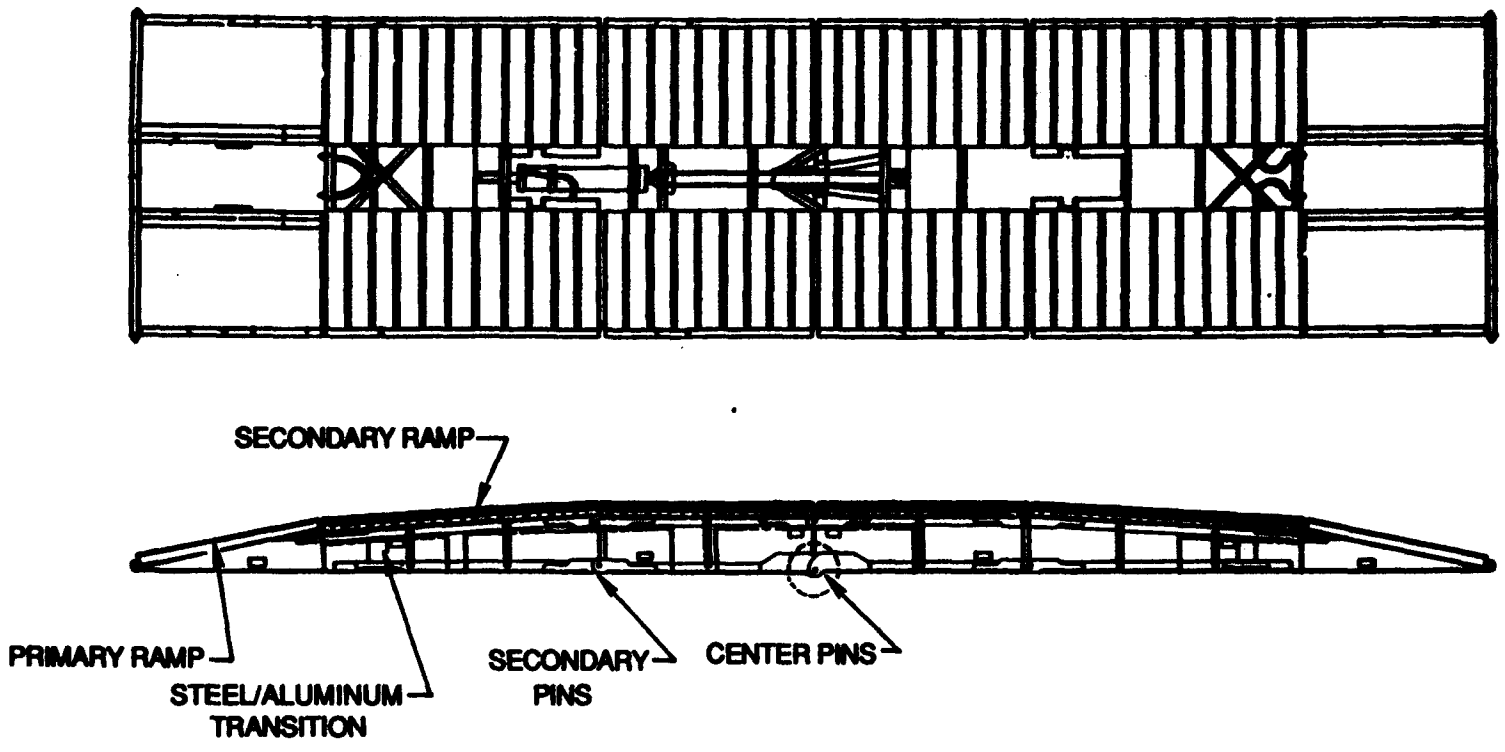

Figure 3. Armored Vehicle Launched Bridge

banks level, a stress of 19.3 Ksi was calculated in the bottom tension chord at a distance of 4 ft from the center hinge. This was the center of the FLI attachment location used for field testing at Aberdeen Proving Grounds (APG, MD) as discussed in Section 6 of this report.

For a configuration of both banks inclined in the same plane, the stress levels can be expected to be similar. For a transverse configuration of the two banks inclined 5 deg opposite to each other for a total bridge twist of 10 deg, test data from other similar bridge experience has shown an expected stress amplification of approximately 25 percent. Thus, a stress of approximately 24 Ksi was calculated for this transverse configuration.

3.3 Static Test Data

Static tests were conducted on the AVLB in April 1990 prior to the commencement of this program. The maximum static loads applied were 140 tons on a span of 60 ft. Strain data from the tension chord, scaled for a span of 53 ft, indicated an average tension chord stress of 17 Ksi, 3 ft from the center hinge, for a level configuration and a load of 70 tons.

Following the crossing tests at APG, MD, static tests were conducted on two AVLBs to determine their residual strength after the fatigue loading. These tests are discussed in detail in Section 7 of this report. Strain data from the tension chord indicated an average tension chord stress of 17.3 Ksi, 3 ft from the center hinge, for a load of 70 tons at a span of 53 ft. During these tests, strain data taken from gauges mounted directly to the bridge at the FLI locations, 4 ft from the center hinge, indicated an average stress of 16.8 Ksi.

3.4 Crossing Tests

Crossing tests were conducted on the AVLB in Spring 90 prior to this program. Numerous crossings were conducted in all three configurations with a 70 ton vehicle at a span of 53 ft. Strain data from the tension chord indicated an average stress of 17.2 Ksi, 3 ft from the center hinge, for a level configuration. Similar strain levels were recorded for the inclined configuration. An average stress of 24.8 Ksi was indicated by strain measurements of the transverse configuration.

During this program, crossing tests were conducted at APG, MD as described in detail in Section 7 of this report. These tests indicated average stresses in the tension chord, 3 ft from the center hinge, for 70 ton crossings over a span of 53 ft of 17.9 Ksi for the level configuration.

During these tests, strain measurements taken directly from the FLI coupons indicated an average stress of 24.6 Ksi, 4 ft from the center hinge, for the transverse configuration.

Table 2 summarizes the available data for the AVLB tension chord.

Table 2. Armored Vehicle Launched Bridge (AVLB) Strain Data for 70 Ton Load on 53 ft Span

Data Source	Loading Type	Loading Condition		
		No. 1 Level	No. 2 Inclined	No. 3 Transverse
APG Crossing Data 4/90	C	1590	1590	2300
Ft. Belvoir 4/10/90	S	1570		
APG Crossing Data 1991				
- FLI Coupons 1/23/91	C			(2280)
- Bridge Gauges 1/3/91	C	~1700		
Ft. Belvoir 5/91				
- Bridge A1-4	S	1650		
- Bridge A1-4 FMI Data	S	(1600)		
Theoretical Prediction	S	1810 (1790)	1810 (1790)	2260 (2240)

C- Crossing
S - Static

Notes:
- All strains are for the Tension Chord, Lower Flange, Top Surface
- Bridge mounted strain gauges are 3 ft from the center hinge
- FLI mounted strain gauges are 4 ft from the center hinge
- Static Analysis is for 3 ft (4 ft) from the center hinge
- Limited configuration No. 2 data from 1990 crossing tests is the same or slightly higher than that of the configuration No. 1 crossings
- Ft. Belvoir tests were conducted with a 60 ft span and data was scaled for a 53 ft span

3.5 Fatigue Critical Locations

There have apparently been no service failures of the AVLB structure attributable to fatigue. However, observed damage from the static and crossing tests provided some insight into the critical locations.

The nominal stress levels in most of the tension chord are not sufficient to result in fatigue failure. However, the areas of high stress concentration along the tension chord are fatigue critical. The center hinge lugs, which react the maximum moment of the bridge loading, are likely fatigue critical locations at both the center pin hole and the rivet points to the tension chord. The tests of April 1990 demonstrated these to be static failure points as shown in Figure 4.

The secondary hinge lugs, which typically see stress levels of approximately 85 percent of those seen by the center hinge under level configuration, may experience higher stresses under some configurations. The static testing of May 1991 demonstrated these lugs as static failure points (Figure 5) and thus potential fatigue critical locations.

The cross members, which carry significant load in a transverse configuration, may also be fatigue critical if significant crossings occur under this configuration. Large cracks were found at APG, MD in the flanges which support these cross members prior to the crossing tests as shown in Figure 6. It was unknown if these cracks were due to previous service crossings or static testing. Regardless, they are clearly a potential fatigue failure point for the bridges. The transition splice from the steel section to the aluminum section may be an additional fatigue area due to high shear stress, numerous fasteners and stiffness and thermal expansion mismatches. No damage has been observed in this area during the static or crossing tests.

3.6 FLI Attachment Locations

Several candidate attachment locations were proposed for the FLI. The large open sections of the AVLB make numerous attachment locations possible based solely on space considerations. Measurements were taken of the AVLB geometry to verify that there was sufficient space for attachment to the upper surface of the bottom flange of the tension chord. As this is the main load-carrying member of the bridge, it was the preferred attachment location to achieve maximum tensile strain. The shear web was also considered as a potential attachment location since adequate space for attachment is available and tensile loading exists.

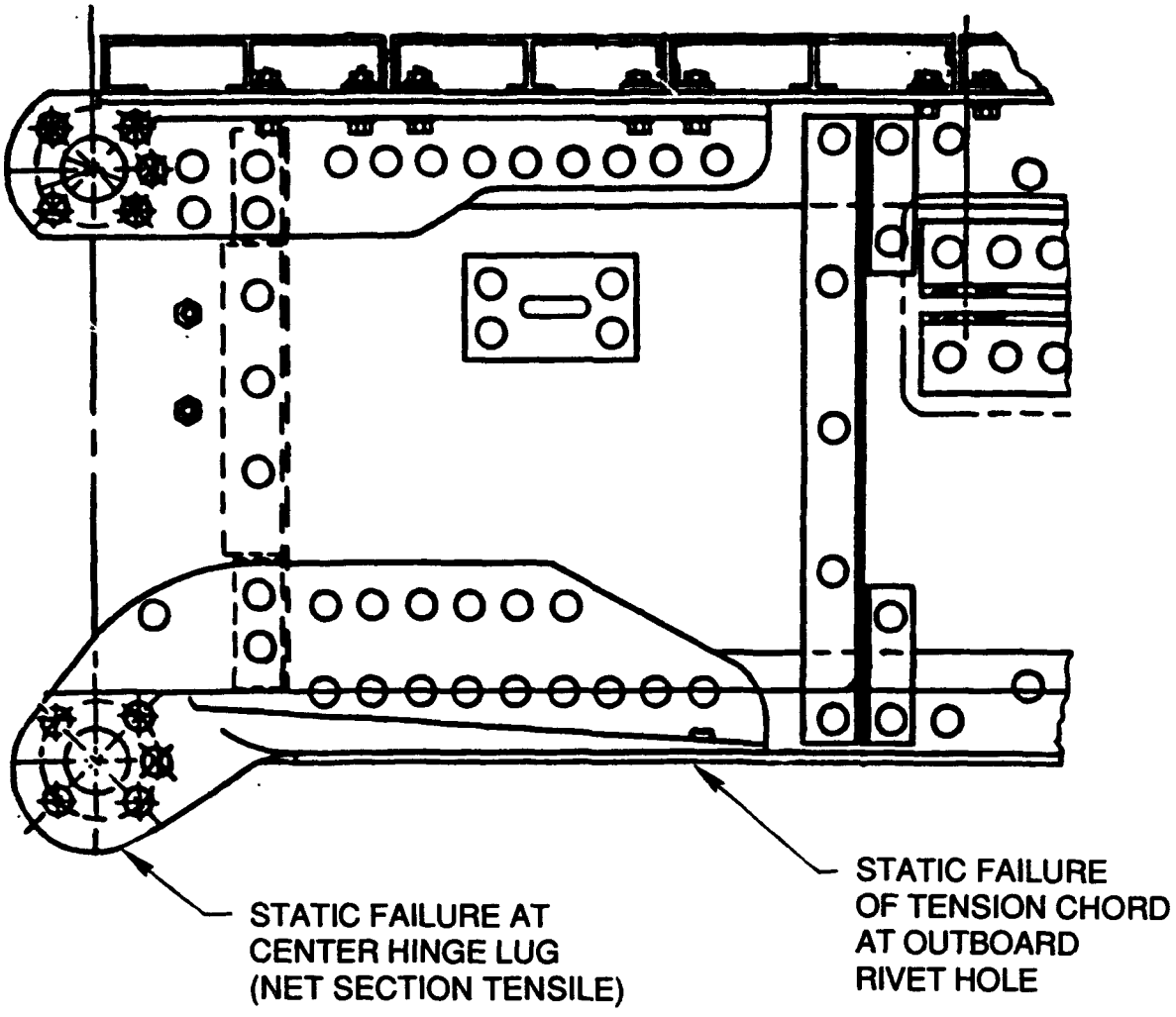

Figure 4. AVLB Static Failure Tests - April 1990

Static and dynamic strain data recorded in various tests of the AVLB were reviewed, as discussed previously. Additional strain data were recorded by Foster-Miller personnel under bridge incremental static loading. The primary selection criteria were adequate space and maximum possible strain without risk of bridge structural damage. The tension chord was selected as the preferable attachment location as the FLI will not interfere with bridge operation and will not degrade the structure provided that a bonded attachment is used. Additionally, this location can be easily accessed for installation and direct inspection. The shear web, which is stressed less than the tension chord, is a viable but not preferable attachment location.

Figure 5. AVLB (A1-4) Static Failure Test - May 1991

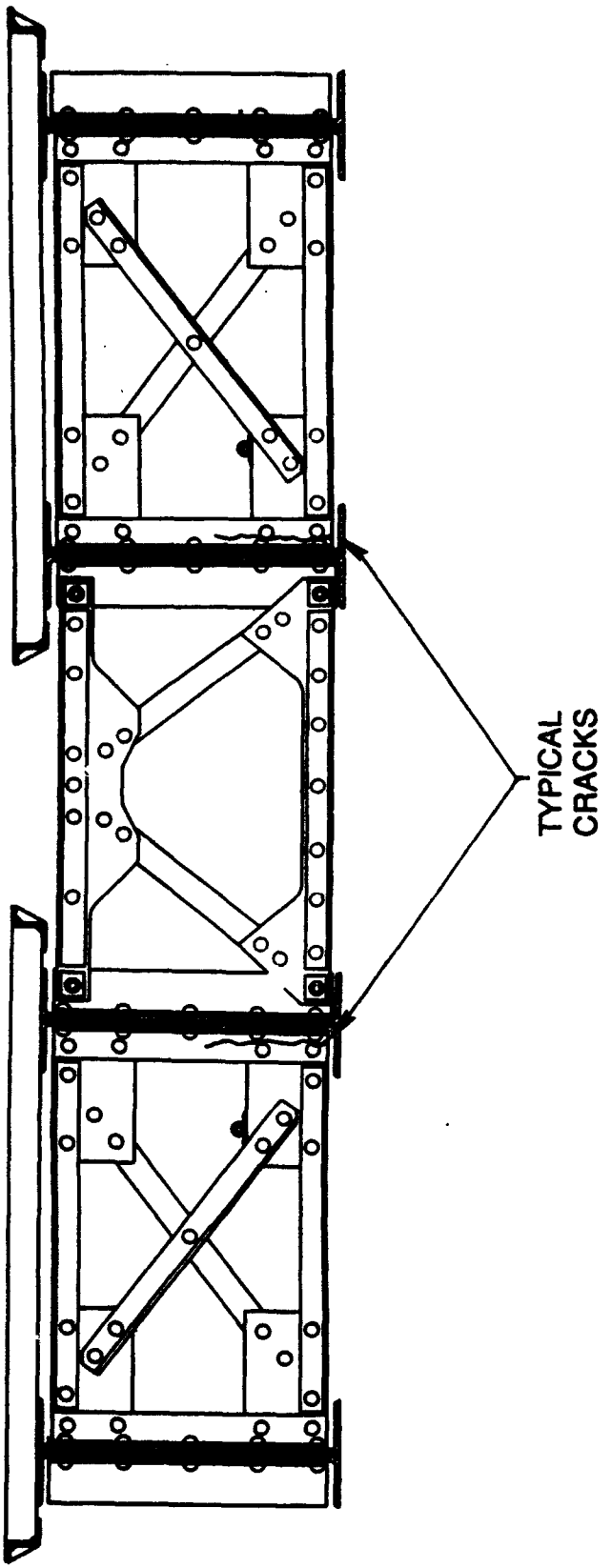

Figure 6. Field Test Observed Cracks AVLB Cross Section

4. COUPON ATTACHMENT

Numerous tests were conducted to evaluate several methods of coupon attachment. Since the AVLB field tests began early in this contract, coupons were bolted to the tension chord as this was the only method to have been proven in the laboratory at that time. Concurrent laboratory testing evaluated bonding to the tension chord. Bolting to the shear web, which was given as an option in the proposal, was not tested as a preferable alternative was identified.

4.1 Bolted Attachment

Numerous tests were conducted to validate the bolted attachment of the FLI coupons. A twelve bolt with doubler plate attachment was used for the laboratory proof-of-concept tests as was shown in Figure 2. This attachment method successfully demonstrated nearly total strain transfer from the parent structure to the FLI coupons.

A six bolt with doubler plate attachment was verified in the laboratory prior to use in the field. A smaller number of bolts was desirable to reduce the damage to the bridge tension chord. This attachment was successfully demonstrated in the laboratory and approved for use in the field proof-of-concept tests.

4.2 Bonded Attachment

4.2.1 Preliminary Bonding Tests

Preliminary tests were conducted using small coupon assemblies to evaluate the five different adhesives which were initially considered. The coupons were mechanically cycled to evaluate their performance under AVLB representative fatigue loading. Thermal cycling was also conducted to give a preliminary indication of adhesive degradation in the environment. As the coupons are expected to be sealed upon application, environmental contamination was not tested. However, further testing of a sealed coupon would be beneficial in a full-scale evaluation to define expected system performance.

4.2.1.1 Test Specimens

The coupon assembly, shown in Figure 7, consisted of a 0.25 in. thick parent coupon made from 6061-T6 Aluminum and a 0.04 in. thick test coupon made from either 2024-T3 or 6061-T6 Aluminum. The test coupon was bonded to the parent coupon at the areas indicated in Figure 7. All bonded surfaces were prepared using the following procedure.

- Degrease material with acetone
- Etch mating surfaces with a solution of ferric sulfate and sulfuric acid
- Wash with alkaline soap
- Rinse and allow to dry.

Coupon assemblies were then bonded according to the manufacturers instructions with heat curing provided by infrared lamps as required. By exception, the specimens bonded with the Ft. Belvoir supplied epoxy were cured in an oven under a precisely controlled temperature of 120°F.

4.2.1.2 Test Facility

Load was applied to the parent coupon in an Instron 8502 tensile test machine using standard wedge grips. Strain transfer from the parent coupon to the test coupon was measured with an axial strain gauge mounted at the center of each coupon. Strain gauges were recorded with an ACRO900 data acquisition system. The test loading configuration is shown in Figure 8.

4.2.1.3 Test Procedure

The test procedure for the small coupon assemblies included static, fatigue, and thermal loading. The static test of strain transfer consisted of loading the assembly in 1,000 lb increments to 7,000 lb (25 Ksi) and measuring the strain in each coupon. While the measured stress levels in the Armored Vehicle Launched Bridge are typically a maximum of 20 Ksi, it was desirable to evaluate performance for higher stress applications. The fatigue loading consisted of cycling the assembly from 1,000 lb to 7,000 lb at a frequency of 1 Hz in 2,000-cycle increments. The thermal cycling consisted of cycling from approximately 10°F to 150°F in 10-cycle increments. Static tests were performed between each increment to monitor strain transfer. Increments were alternated until 10,000 fatigue cycles (the design life of the AVLB) and 30 thermal cycles were completed.

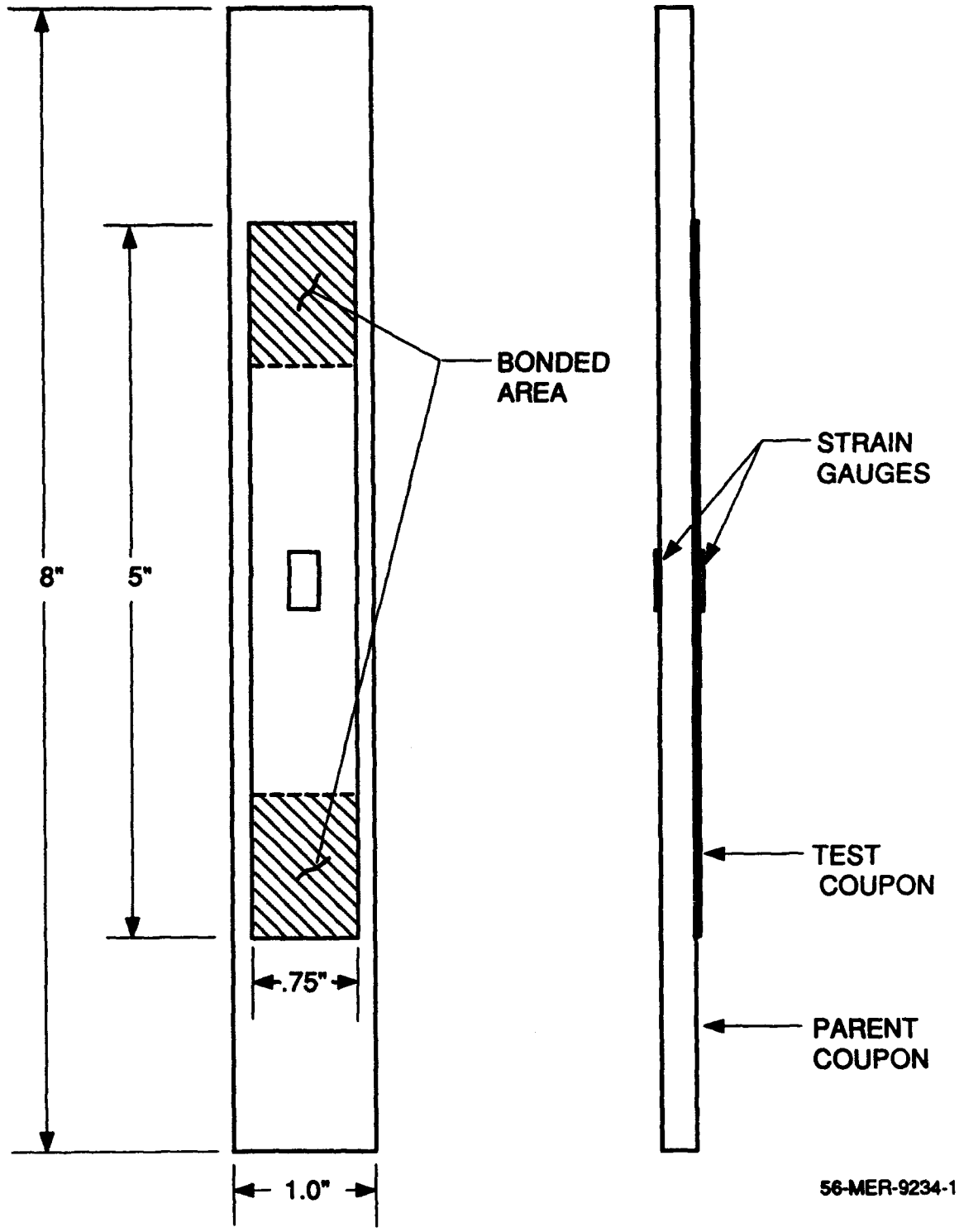

Figure 7. Preliminary Bonding Test Assembly

Figure 8. Small Coupon Assembly Test

4.2.1.4 Test Results

More than 20 coupon assemblies were tested in this preliminary evaluation of their suitability for FLI attachment. A summary of all testing is provided in Table 3. The following subsections present the results for each of the five adhesives evaluated.

Martin Marietta Laboratories (MML) Epoxy

This three-part epoxy was developed by MML under a contract to the Ft. Belvoir RD & E Center, to be used for structural repair of bridges. A sample of the adhesive was provided to Foster-Miller by Ft. Belvoir. Four assemblies were bonded for testing. Two were cured at room temperature for seven days and two were cured at 120°F for two days. Static tests of all four assemblies indicated an average strain transfer of 85 percent with negligible difference between the room temperature cure and the 120°F cure specimens. Fatigue tests were then conducted on one assembly of each cure method. Failure occurred in the two specimens after 972 and 990 cycles had been applied. This could be due to inadequate surface preparation and therefore, further work was planned with the collaboration of MML to study the problem. Four small coupon assemblies were prepared by MML for additional testing.

Table 3. Preliminary Bonding Test Results

Adhesive	Cyclic Tests	Failures	Avg Initial Strain Transfer	Avg Final Strain Transfer
MML Epoxy	2 4*	2 0	85.0 78.9	N/A 78.6
Loctite 430	2	2	83.1	N/A
Tra-Bond 2129	3	3	80.0**	N/A
Tra-Bond 2143D	3	0	83.4 (84.9)***	74.2 (78.4)
Devcon Aluminum Putty	3	0	81.4	71.0

* MML prepared coupon assemblies
** One assembly failed under initial static loading
*** Discounting specimen cooled by icewater submersion

The manufacturer prepared coupon assemblies utilized a more extensive surface preparation. The mating surfaces were mechanically roughened and then etched in a phosphoric acid bath with 10V across the solution. The bond line was significantly thicker than that of the previous coupon assemblies. The epoxy was heat cured, cooled, and then post-cured in a controlled environment.

Tests with these assemblies indicated slight bond degradation at most after 10,000 mechanical and 30 thermal cycles. The performance of this epoxy, once proper bonding was accomplished, was satisfactory and comparable to the other adhesives tested in the laboratory.

Loctite 430

Loctite 430 is a commercially available cyanoacrylite "superglue" which cures extremely quickly at room temperature to form a hard, brittle bond. Static tests of two assemblies indicated an average strain transfer of 83 percent. Fatigue tests conducted on these assemblies caused failure after less than 500 cycles. No further testing with Loctite 430 was conducted in the laboratory.

Trabond 2129

Trabond 2129 is a commercially available two-part epoxy manufactured by Tra-Con, Inc. Although this epoxy could cure at room temperature, these assemblies were cured for 4 hr at 150°F. Three assemblies were initially manufactured for evaluation. Assembly A failed under static load at 4000 lb (14 Ksi). Assembly B was statically tested to 7000 lb and fatigue tested for 2000 cycles. Following cycling it demonstrated a strain transfer of 71 percent. Failure occurred after 1282 additional cycles. Assembly C was statically tested to 7000 lb and failed in fatigue testing after 84 cycles. No further testing with Trabond 2129 was performed in the laboratory.

Devcon Aluminum Putty

Devcon aluminum putty is a commercially available two-part aluminum filled epoxy manufactured by MSC/Dancorp. The thermal expansion properties of this epoxy, due to the aluminum fill, are designed for this application. This epoxy could cure at room temperature; however, these assemblies were cured for 4 hr at 150°F. Three assemblies were manufactured for evaluation. All three assemblies were tested for the complete procedure of 10,000 fatigue cycles and 30 thermal cycles. Static tests performed after each increment showed an initial average strain transfer of 81.5 percent with a degradation to a final average strain transfer of 71 percent.

Post-test inspection did not reveal any bond degradation. The data define an average strain transfer percentage of 76.2 ±5.0 which may be acceptable for FLI attachment. The relative ease of application also makes this epoxy a good candidate for the present application.

Trabond 2143D

Trabond 2143D is a commercially available two-part aluminum filled epoxy manufactured by Tra-Con, Inc. These assemblies were cured for 4 hr at 150°F. Three assemblies were manufactured for evaluation. All three assemblies were tested for the complete procedure of 10,000 fatigue cycles and 30 thermal cycles. Static tests performed after each increment showed an initial average strain transfer of 84.9 percent with a degradation to a final average strain transfer of 78.4 percent in assemblies B and C. Assembly A was exposed to water during thermal cycling and saw a degradation in strain transfer to 66 percent.

Post-test inspection did not reveal any bond degradation. Assembly A tests showed an apparent sensitivity to moisture degradation. Therefore, an effective sealing method to isolate the adhesive from moisture contamination needs to be defined.

The data defines an average strain transfer percentage of 82.7 ±2.5 which should be acceptable for FLI attachment. This epoxy is packaged in pre-measured quantities in a two section package as shown in Figure 9. It is well-designed for ease of application in the laboratory or the field. This capability coupled with its strain transfer rate made it useful in full-scale laboratory testing.

4.2.2 Full-Scale Bonding Tests

4.2.2.1 Test Specimens

Full-scale bonding tests were conducted using an assembly similar to that used with the bolted connections in Phase I of this program. This assembly, shown in Figure 10, consisted of a 0.25 in. thick parent coupon made from 7075-T6 Aluminum and two 0.04 in. thick precracked FLI coupons made from 2024-T3 and 6061-T6 Aluminum. The test coupons were bonded to the parent coupon at the areas indicated in Figure 11. All bonded surfaces were prepared using the same procedure defined for the preliminary bonding tests. Tra-Bond 2143D epoxy, cured for 4 hr at 160°F under heat lamps, was used for all test assemblies. Two Krak-Gages were bonded to each of the FLI coupons to evaluate their performance, as discussed in detail in Section 5.3.

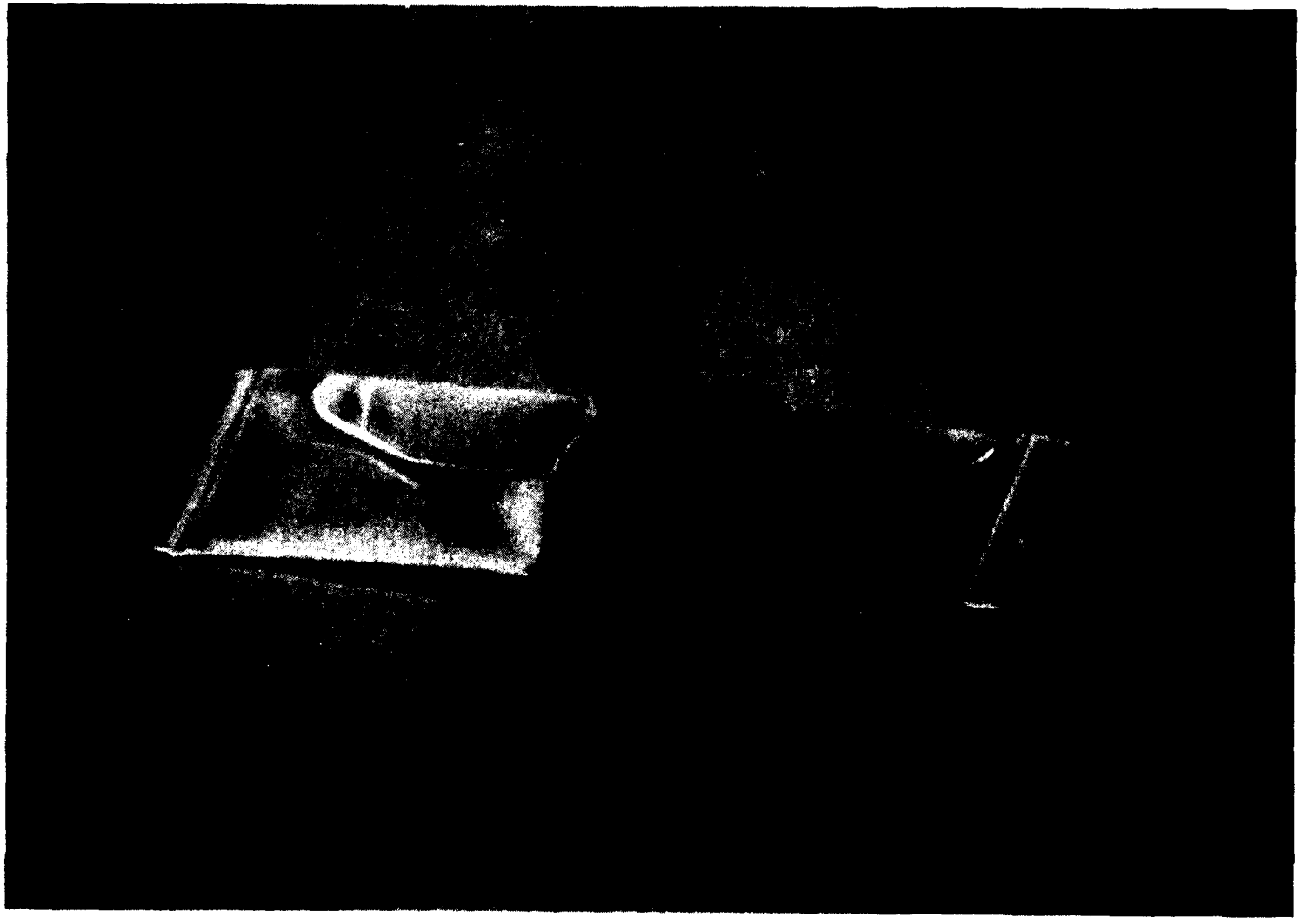

Figure 9. Tra-Bond 2143D Pre-Measured Package

Figure 10. Full-Scale Bonding Test

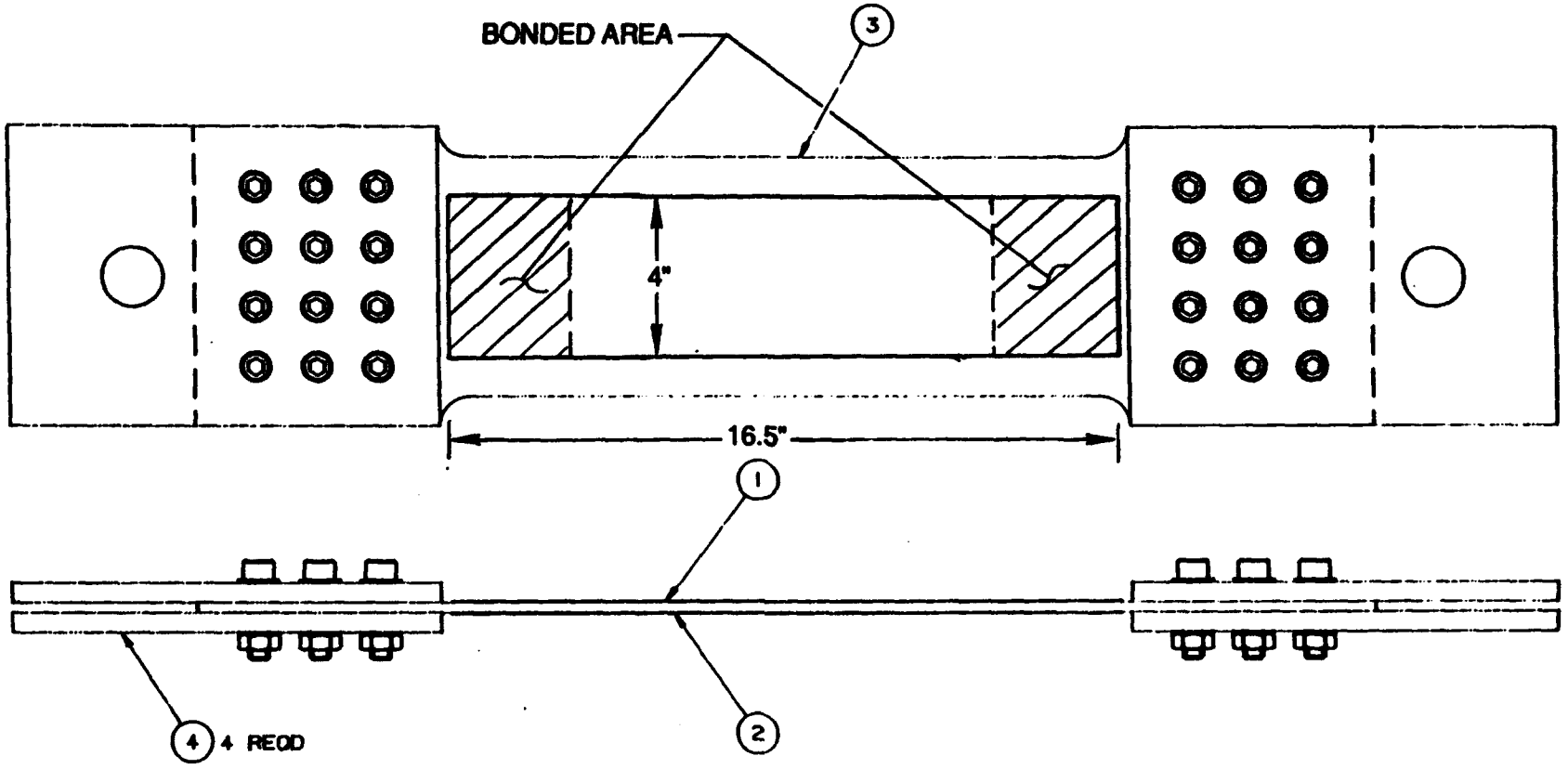

4	4	9043004	SIDE PLATE-2	FMI
3	1	9043003	TEST COUPON	FMI
2	1	9043001-2	FLT COUPON	FMI
1	1	9043001-1	FLT COUPON	FMI

PARTS LIST

FOSTER-MILLER, INC.

COUPON ASSY

C 30233

MER9043 1/2

Figure 11. Full-Scale Bonding Test Assembly

4.2.2.2 Test Facility

Load was applied to the parent coupon in an Instron 8502 tensile test machine using single pin clevis grips. Strain transfer from the parent coupon to the test coupons was measured with an axial strain gauge mounted at the center of each coupon. Strain gauges were recorded with an ACRO900 data acquisition system.

4.2.2.3 Test Procedure

The test procedure consisted of cyclically loading the assemblies at a precisely controlled stress range. In order to conduct the maximum number of comparative tests for the purpose of coupon size optimization, discussed in Section 8, all tests were performed at a constant stress range. Phase I testing of the FLI indicated that data for different stress levels can be related with reasonable accuracy over a range of approximately 15 to 25 Ksi.

4.2.2.4 Test Results

Five assemblies were tested to evaluate the bonded attachment and the performance of the Krak Gage measurement system. The results of these tests are summarized in Table 4 and complete test data are provided as Appendix A. Stress histogram calculations from assemblies C and E show good agreement with the applied number of cycles and typically indicate a 20 percent reduction in stress due to the bonded attachment.

Assembly D demonstrated comparable crack growth in the 6061-T6 coupon but significantly retarded crack growth in the fully bonded 2024-T3 coupon. This test is discussed in detail in subsection 8.2.

The bonded attachment performed well. Since the coupon cannot slip, as it did in field testing with bolted attachments, bonding provides a major system improvement. The 2024-T3 coupon in Assembly B was significantly disbonded prior to parent coupon failure. However, more than 14,000 cycles had been applied to the assembly before any disbonding occurred. The performance of the Krak Gage system was excellent, as discussed in detail in subsection 5.3. Assembly E demonstrated the possibilities for effective coupon size reduction, as discussed in detail in subsection 8.3.

Table 4. Stress Histogram Calculations

Assembly B				
Applied		Calculated		Comments
Cycles	Stress	Cycles	Stress	
0				
12500	18.0	13400	14.3	
15300	18.0	36200	11.7	2024-T3 Coupon 50% Disbonded
16700	18.0	43200	11.5	2024-T3 Coupon 70% Disbonded
Assembly C				
0				
1300	20.0	1000	16.4	
3000	20.0	2400	17.3	
4000	20.0	4100	17.0	
5000	20.0	5500	16.2	
6600	20.0	6500	16.5	
8000	20.0	7800	16.5	
9000	20.0	9100	16.1	
10000	20.0	9700	16.1	
12000	20.0	11700	15.8	
13000	20.0	12400	15.7	
14000	20.0	13700	15.4	
15000	20.0	14700	15.3	
16000	20.0	15200	15.3	

5. AUTOMATED CRACK MEASUREMENT

Three systems were considered for automated crack measurement of the Fatigue Life Indicator coupons. The previous work used visual crack measurement under a graduated microscope. While this system is common practice for laboratory testing, it is labor intensive, especially in the field. The FLI should be easily readable by minimally trained personnel after its installation. The potential drop method, crack growth ladder gauges, and the Krak-Gage system were evaluated for this application.

5.1 AC Potential Drop

5.1.1 General Description

The potential drop method involves passing a current directly through a conductive test specimen with leads attached to the specimen on either side of the crack. As the crack length increases, the impedance measured will increase proportionately due to the longer path which the current must follow to circumvent the crack face. Two methods are available, namely AC and DC potential drop.

For this application, the preferable method would be AC potential drop (ACPD). The most significant advantage of DCPD is its ability to penetrate the specimen and provide the average through depth crack length. Thus, any crack tunnelling or other subsurface growth patterns would be taken into account. However, with the thin coupons used in this system, these effects are insignificant and surface crack measurement is equally representative. ACPD requires a much lower current level (typically 3A) to achieve acceptable signal to noise ratios. Thus, crack tip heating effects, which can result from high current levels (typically 50A for DCPD), are minimized. Also, in ACPD, output increases with crack growth and decreases with plasticity while both result in output increase in DCPD. This results in higher accuracy slow crack growth measurements using ACPD.

5.1.2 Evaluation

Although the basic theory in this method is sound, several problems were identified in our evaluation. A review of the literature available on ACPD showed that extensive laboratory testing has been conducted to refine this method. These tests have shown that under carefully controlled

laboratory conditions acceptable crack measurement can be made. However, even under these conditions, the impedance of the lead wires can present severe limitations. The initial connection of the lead wires to the specimen must be done with extreme care to ensure impedance consistency between specimens. These wires cannot be disconnected from the data acquisition system during testing as the changes in lead impedance due to reconnection will typically mask the changes due to crack growth. Problems can also result from the changing impedance due to movement of the wires without disconnection.

The temperature fluctuations found outside of a laboratory environment can alter readings as specimen impedance varies with ρ and μ which are temperature dependent. System calibration can also be difficult as the particular specimen geometry must be calibrated and minor production variations can result in significant changes. Additionally, current bridges are constructed from conductive materials. The FLI coupons would need to be electrically isolated from the bridge to prevent any crossover effects.

The extensive literature available on this method indicated that the method is too involved for field use. ACPD was not further considered as a remote crack monitoring system for the FLI.

5.2 Ladder Gauges

5.2.1 General Description

The ladder gauge method provides electronic crack growth measurement using microwire gauges which break as the crack propagates. The two gauges tested in this program are shown in Figure 12. The gauges are directly bonded to the surface of the FLI coupon in front of the crack tip. As the crack propagates through the coupon, the gauge resistance increases as the microwire "rungs" are broken. This stepwise change in resistance provides a digital indication of crack length with a resolution dependent on the wire pitch (spacing).

5.2.2 Laboratory Tests

A total of seven tests were performed on the two different ladder gauges. The gauges were mounted on FLI coupons which were load cycled on an Instron 8502 tensile test machine. The load was introduced directly to the coupon with no parent structure, as shown in Figure 13. Stress cycles of 20 Ksi were applied at a frequency of 1 Hz.

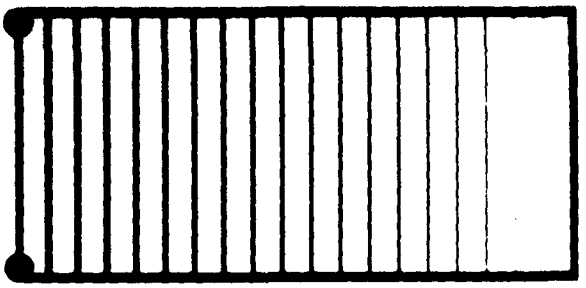

TYPE A

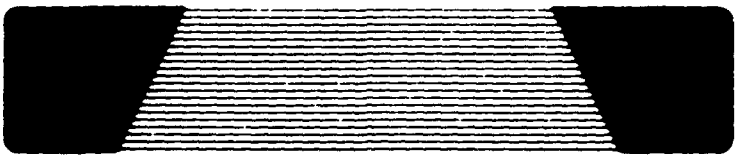

TYPE B

Figure 12. Crack Growth Ladder Gauges

Gauges were bonded directly to the coupon, with a standard cyanoacrylite adhesive used for strain gauges. The gauge circuit is wired with the gauge in parallel with a 50Ω shunt resistor (actually a 50.6Ω was used for these tests). The resistance was measured with a hand-held Fluke DMM. The coupons were cycled and the crack propagated through the gauge.

5.2.3 Test Results

Type A

Two tests were conducted using Type A gauges which are designed with variable "rung" wire gauge to yield uniform resistance steps as the crack propagates. These gauges have a rung pitch of 0.080 in. and a total length of 1.50 in. The results of these tests are shown in Figure 14. Both tests were halted prior to crack propagation throughout the entire gauge, as shown in Figure 15, due to some disbonding of the gauges near the crack tip.

Two problems surfaced during these tests. The Type A gauge experienced changes in the resistance measurements due to partial contact of the ends of failed rungs during crack closure.

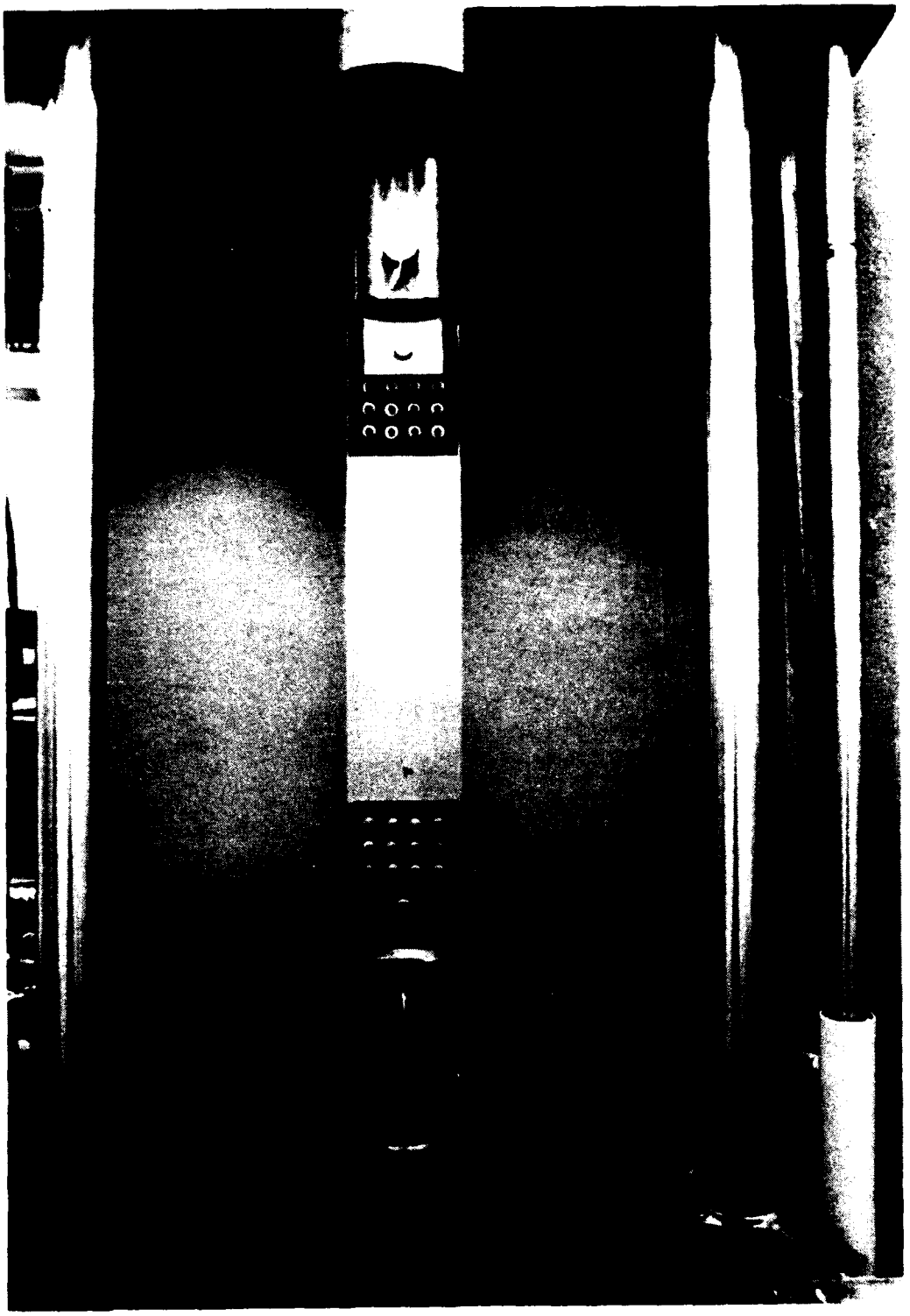

Figure 13. Ladder Gauge Test Setup

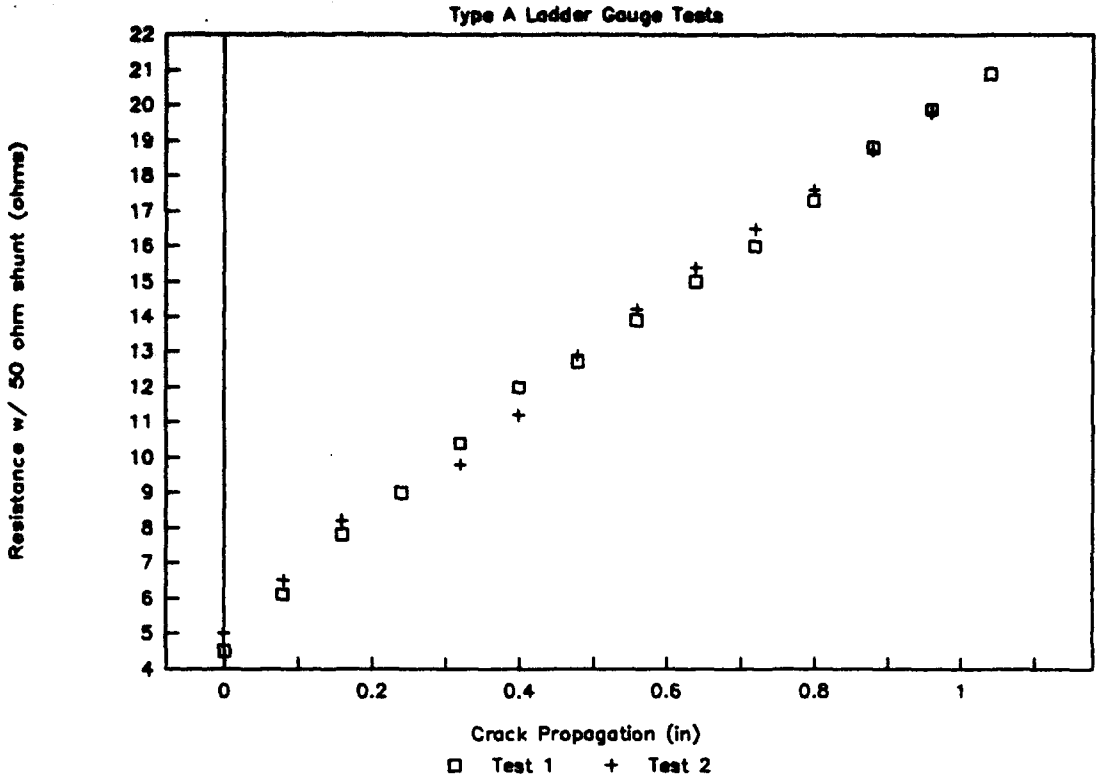

Figure 14. Fatigue Life Indicator Phase II, Type A Ladder Gauge Tests

Also, the significant scatter observed in the output of the two tests made it difficult to relate a discrete resistance to a crack length. Thus, a second type of gauge was tested to alleviate these problems.

Type B

Five tests were conducted using Type B gauges which are designed with constant "rung" wire gauge to yield increasing resistance steps as the crack propagates. These gauges have a rung pitch of 0.010 in. and a total length of 0.20 in. The results of these tests are shown in Figure 16. All five tests continued crack propagation throughout the entire gauge length, as shown in Figure 17.

The problems observed in the Type A tests were generally not found in these tests. As can be clearly seen in the plot, the scatter between the five tests is very small. Thus, a discrete resistance measurement can be related to a crack length. There was no disbonding of the gauges observed. Also, due to the smaller rung wire gauge, contact apparently did not occur between the ends of failed rungs as in the previous tests. Although there is still concern over resistance changes due to disconnection of lead wires, these preliminary tests seem to indicate that this

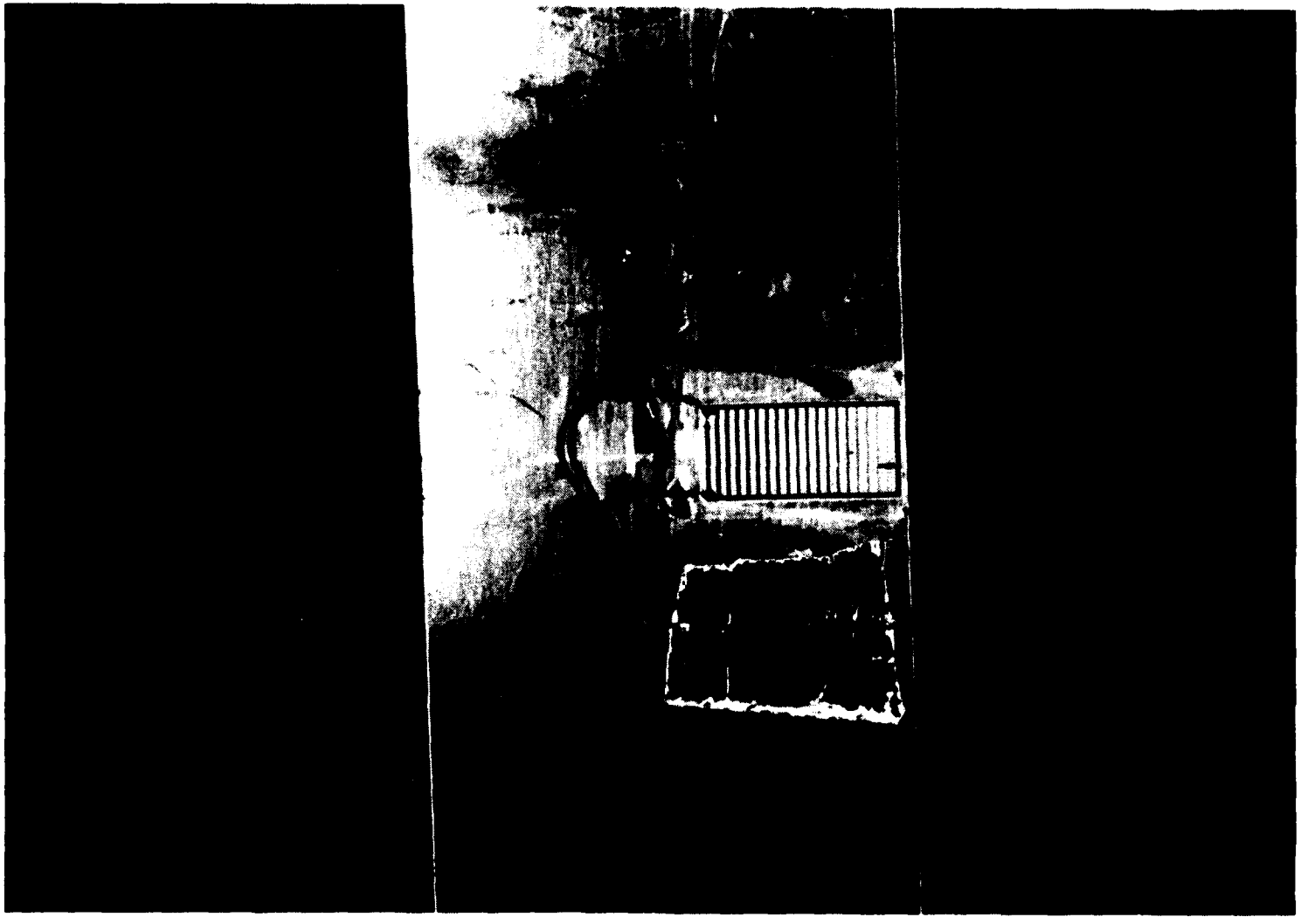

Figure 15. Type A Gauge

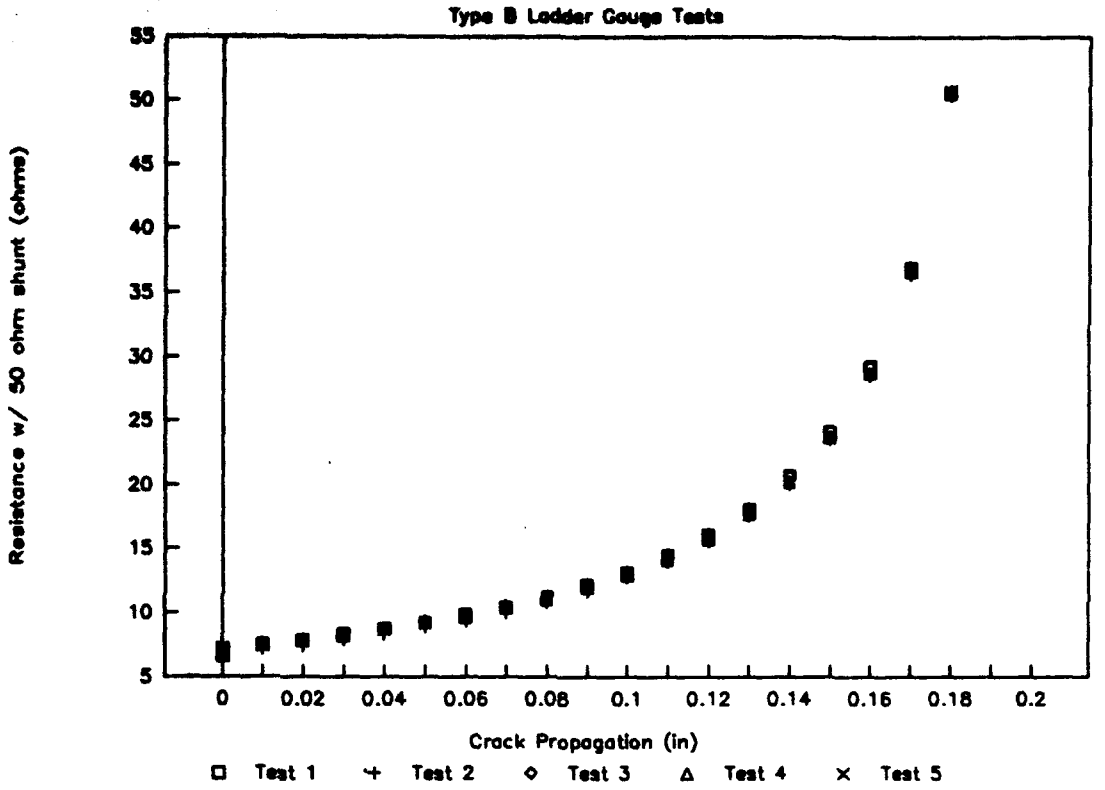

Figure 16. Fatigue Life Indicator Phase II, Type B Ladder Gauge Tests

is an acceptable method of remote crack measurement if the resolution of 0.010 in. is deemed acceptable.

5.3 Krak Gage System

5.3.1 General Description

The Krak Gage system provides crack growth measurement electronically using an indirect DC potential drop method. A thin foil Krak-Gage is bonded directly to the test specimen and the crack propagates through the gauge as it propagates through the test specimen.

The change in the resistance of the gauge is precisely measured by a Fractomat data acquisition device. This two-channel instrument contains precision constant current sources for excitation as well as signal conditioners and amplifiers to process the input. The two calculated crack lengths are displayed on the instrument front panel. This system, which is in wide use in fatigue laboratories, provides several significant advantages over other crack measurement devices.

Figure 17. Type B Gauge

- Crack length is directly displayed. This significantly reduces operator error.

- It is a remote measurement system requiring no visual contact with the specimen and thus permitting permanent sealing of the specimen.

- The system can be disconnected from the specimen and reconnected later with no loss in accuracy. Consequently, one reading unit can be used to separately interrogate numerous gauges.

- The continuous foil gauge has essentially infinite resolution.

The disadvantages associated with this system are as follows:

- The initial cost of the Fractomat data acquisition system is relatively high (≈$7,000)

- The Krak Gages must be properly applied during coupon fabrication

- Standard 110 VAC power must be available to operate the system when a reading is to be made

- The coupon will be completely sealed from visual inspection of the cracks.

5.3.2 Laboratory Tests

Five full-scale bonding tests were conducted, as discussed in subsection 4.2.2. A total of 17 Krak Gages were applied for testing of this measurement system. Two gauges were applied to each FLI coupon in order to measure the total tip-to-tip crack length, as shown in Figure 18. The system experienced a minor initial hardware problem which resulted in the data from the two gauges on Assembly A being unrepresentative. However, 15 gauges provided adequate data for system evaluation. The data from these gauges are presented in Appendix A.

5.3.3 Test Results

The Krak Gage tests successfully demonstrated five key aspects of system performance.

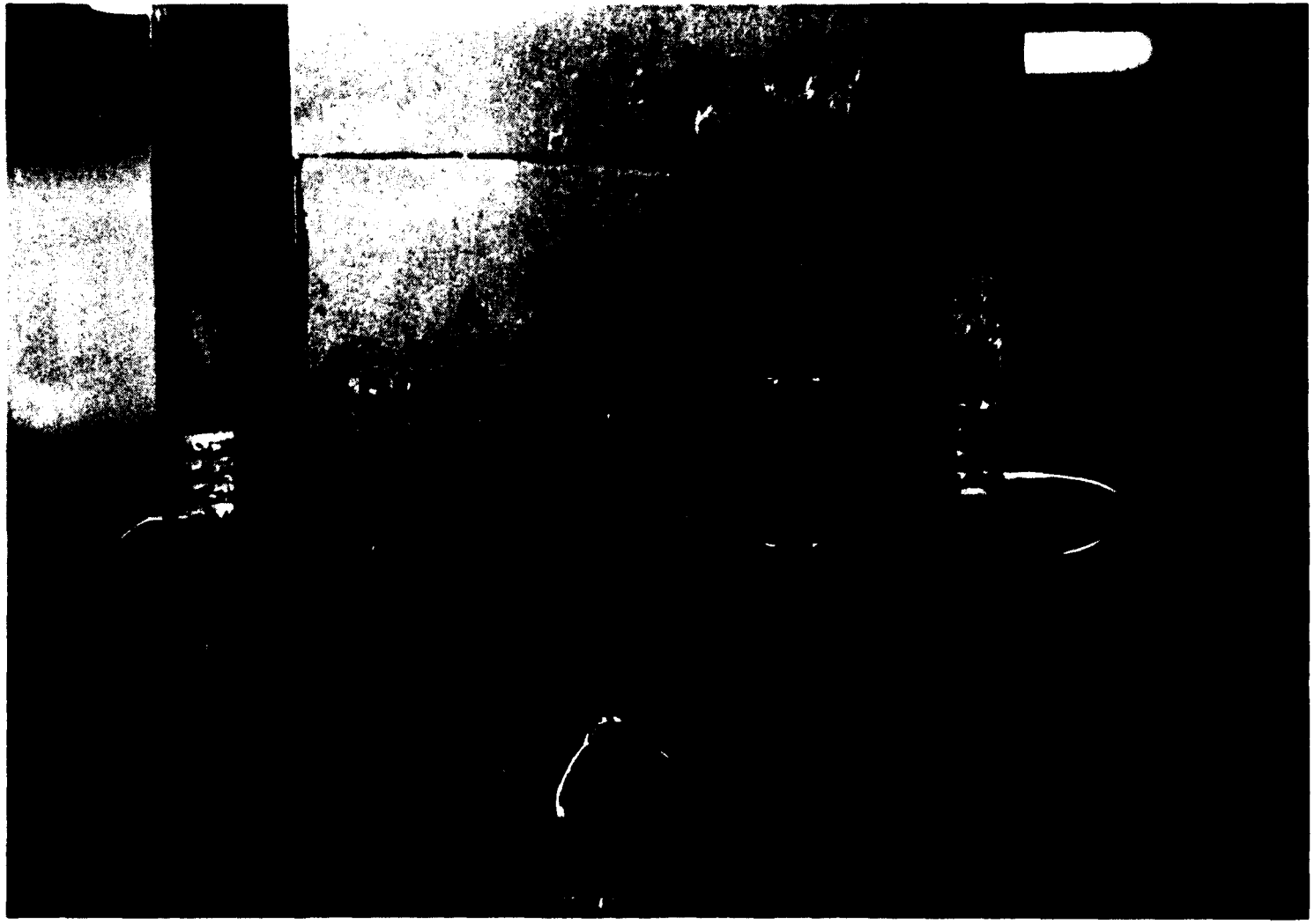

Figure 18. Krak Gages

Accuracy

A comparison of the Krak Gage readout to precision optical measurements made with a graduated microscope is presented as Figure 19. Agreement was excellent with any error likely due to some difficulty in correctly identifying the crack tip during optical measurement.

Resolution

As stated previously, the Krak Gage offers very fine resolution. Since the gauge itself is an analog indicator, the resolution is dependent on the recording device. For the 30 mm gauges typically used in these tests, the minimum displayed resolution of the Fractomat is 0.01 mm (0.0004 in.). The Fractomat also can display the peak readout of the gauge to eliminate any error due to crack closure during cyclic loading.

Crack Closure Effects

Four gauges of different crack lengths were tested statically to quantify the effects of crack closure as shown in Figure 20. The applied stress required to overcome closure was proportional to the crack length. The error associated with crack closure may be significant with extremely

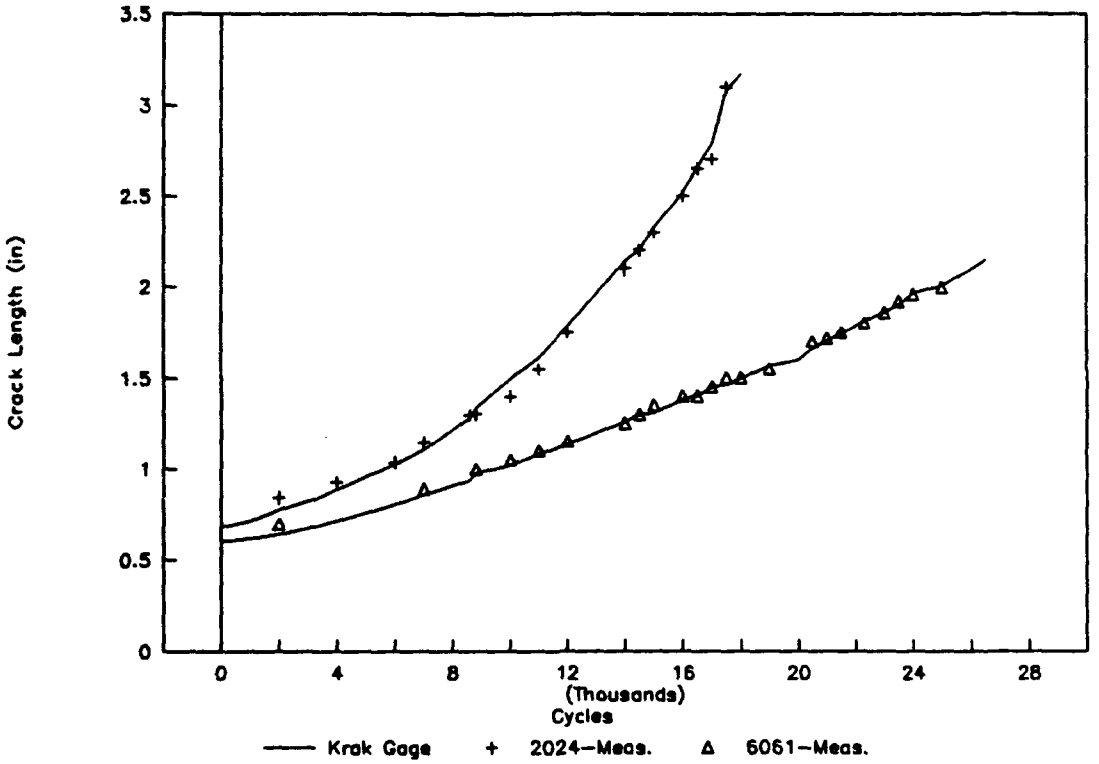

Figure 19. Krak Gage Comparison to Optical Measure

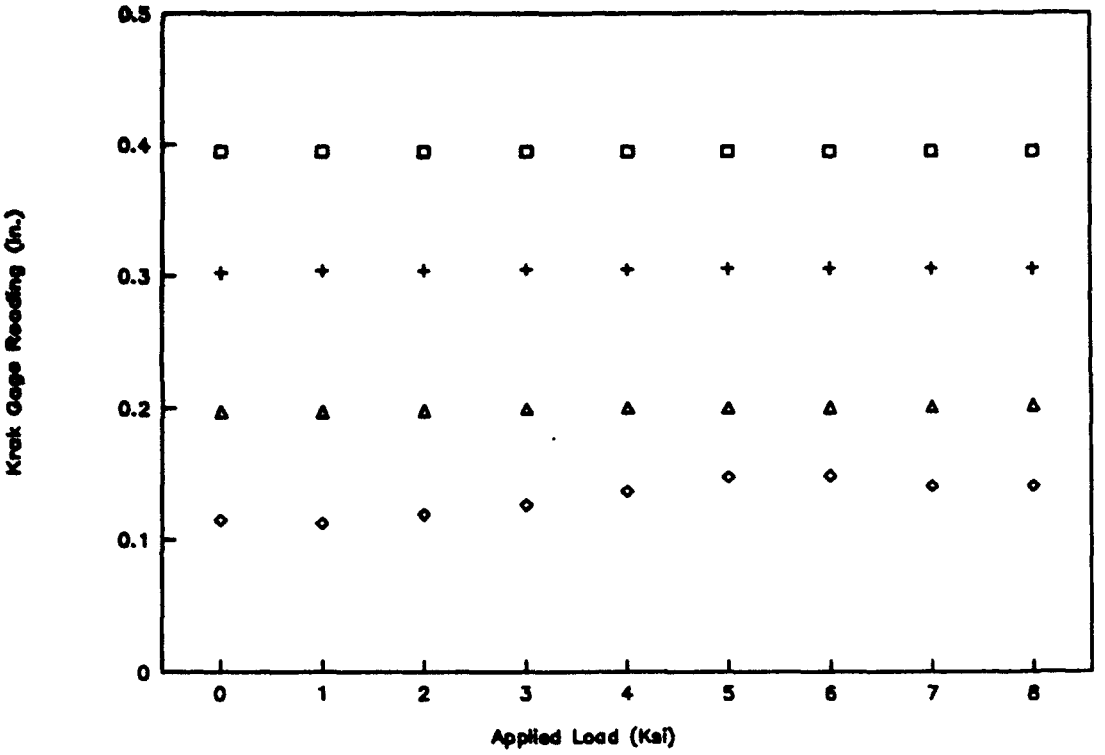

Figure 20. Crack Closure Effects

small crack lengths. However, the stress due to the dead weight of the bridge was sufficient to overcome closure effects in all but the smallest cracks.

Gauge Attachment

All of the gauges tested remained fully bonded to the FLI coupons through the duration of testing, unlike the ladder gauges, which sometimes disbonded near the crack tip. The Krak Gage bonding integrity was found to be excellent when the manufacturer-recommended epoxy was used.

System Disconnect

The Fractomat measurement system will not be continually connected to the gauges in actual FLI field operation. In order to be cost-effective, one Fractomat must be usable for reading numerous different FLI units. Thus, it was important to demonstrate system stability.

Throughout all testing, the Fractomat was connected to the gauges through standard cannon plugs. These plugs were disconnected and reconnected at numerous times throughout the testing.

No errors were recorded due to these actions. Since the system maintains a pre-set, constant current, changes in system resistance were automatically compensated and the output was not adversely affected.

6. FIELD INSTALLATION OF THE FATIGUE LIFE INDICATOR

6.1 Coupon Attachment Method

Due to the field testing time constraints, alternate coupon attachment methods had not been sufficiently tested in the laboratory. Thus, an adapted version of the bolted attachment method utilized successfully in the previous laboratory tests was considered for this application. A pattern of three rows of two bolts with a doubler plate on each end of the coupon was tested in the laboratory and found to be sufficient for attachment.

The calculated stress in the tension chord at the proposed FLI attachment location was expected to be a maximum of 20 Ksi for the field test loadings. A two-bolt row results in a 5 percent cross section area reduction of the bottom flange of the tension chord and approximately a 3 percent increase in the net section stress. Even with consideration of the hole stress concentration factor of 3, this attachment should present no problems over the useful fatigue life of the bridge. Additionally, it was determined that the coupon attachment would not interfere with the planned operation of the bridge during the crossing tests. Thus, this attachment method was approved for use in the field proof-of-concept tests by Ft. Belvoir personnel.

6.2 Field Installation

Two sets of Fatigue Life Indicator coupons were attached to each of two Armored Vehicle Launched Bridges (AVLB) at Ft. Belvoir, VA. Two sets were prepared for a standard useful life of 10,000 cycles and denoted as -10. Two more sets were prepared for a useful life of 2,000 cycles and denoted as -02. This was accomplished by cycling the -02 sets to longer initial crack lengths for a target useful life of 2,000 cycles to provide greater accuracy during the planned field tests. One set of each type was attached to each of the bridges.

The coupon sets were attached to the AVLBs at the locations summarized in Table 5 and Figure 21. Individual coupons of a set were mounted on opposite sides of the center hinge at an end location 41 in. from the center pin, as shown in Figure 22. The coupons were then sealed with silicone to prevent moisture and dirt penetration. The coupon locations were also padded for additional protection during the bridge transport to Aberdeen Proving Grounds, MD (APG) for the crossing tests. Figure 23 shows a mounted and sealed coupon.

Table 5. Fatigue Life Indicator Field Proof-of-Concept Tests

Bridge	Coupon Set Number	Coupon Set Type	Attachment Location Number	Coupon Material	Initial Crack Tip-to-Tip
A1-3	1	-10	1	2024-T3	0.500
			2	6061-T6	0.500
	3	-02	3	2024-T3	0.800
			4	6061-T6	0.900
A1-4	2	-10	1	2024-T3	0.500
			2	6061-T6	0.500
	4	-02	3	2024-T3	0.800
			4	6061-T6	0.900

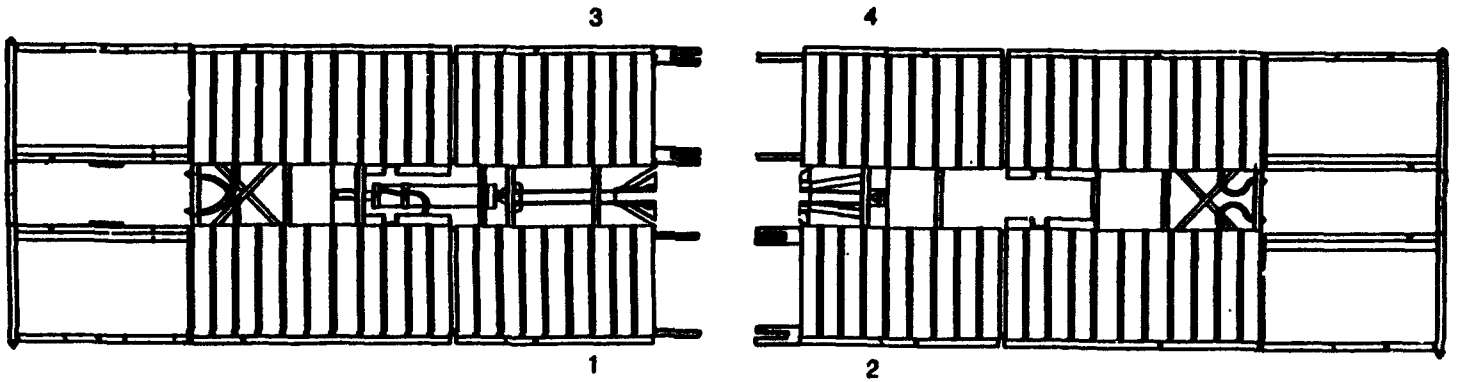

NOTE: LINKS ARE NOT TO SCALE

Figure 21. FLI Attachment Locations

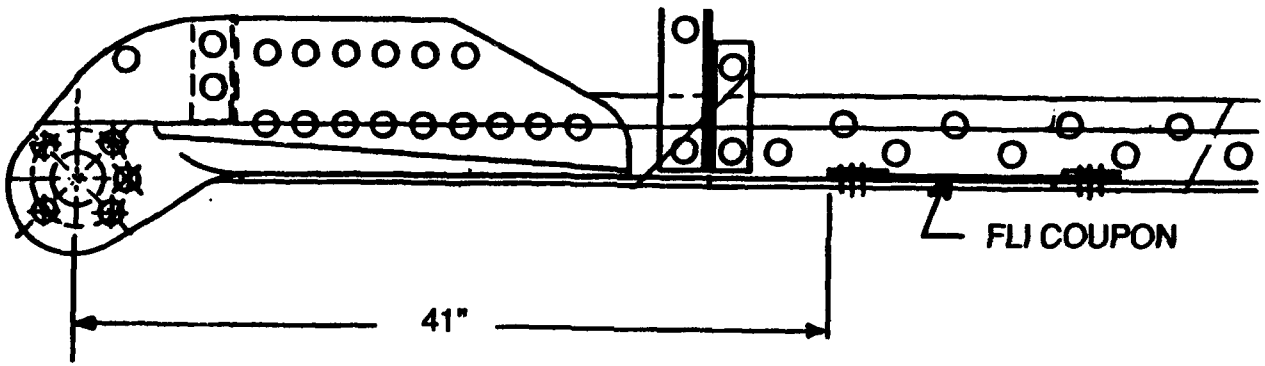

Figure 22. Individual Coupon Mountings

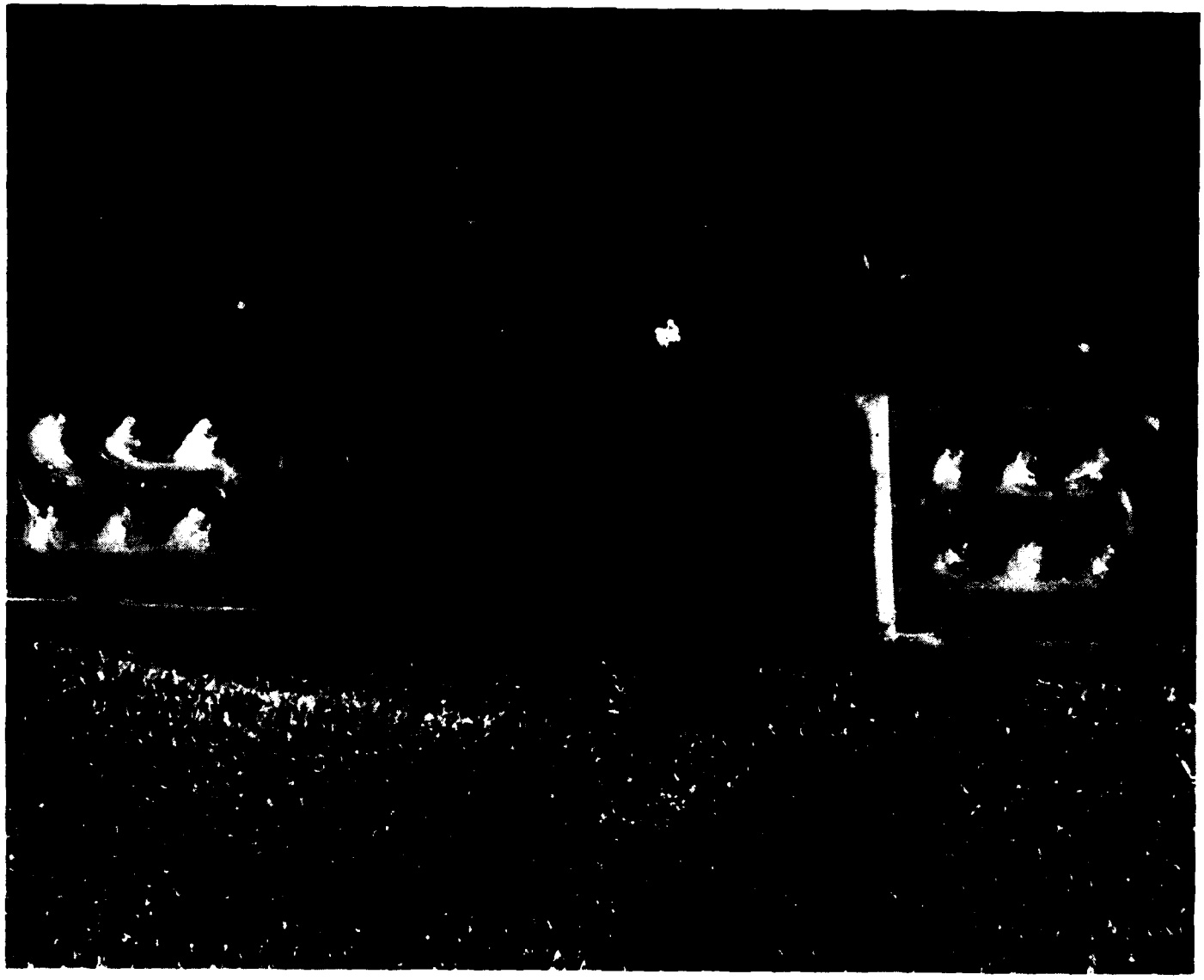

Figure 23. FLI Coupon Installed on the AVLB

7. FIELD PROOF-OF-CONCEPT TESTS

7.1 Crossing Tests at Aberdeen Proving Grounds

On-site test monitoring was made at Aberdeen Proving Grounds (APG), MD during the AVLB crossing tests to support the FLI field proof-of-concept testing. Crack lengths and strains were recorded. The data were collected and analyzed over four separate periods.

7.1.1 First Period - 26 Nov 90 to 22 Jan 91

The condition of all of the FLI coupons following transport of the bridges from Ft. Belvoir, VA to APG was checked. Seven of the eight coupons appeared to be in excellent condition. One coupon (Bridge A1-4, Set 2, Location 2) appeared to be slightly bulged in the center. Few crossings had been made on either bridge so no visible crack growth had occurred.

Strain gauge data were to be acquired from all eight coupons during crossings to evaluate the strain transfer from the bridges to the coupons. However, adverse weather severely hampered instrumentation hook-up. Data were recorded for 10 crossings of Bridge A1-3 which was configured with a 53 ft span, 8 percent incline, and 70T vehicle crossing. The data from coupon set 1 are presented in Table 6. These data indicated an average stress cycle in the tension chord of approximately 24 Ksi.

Damage to the bridges was also observed. Cracks in the cross brace attachment flanges were found by APG personnel prior to the crossing tests. As a result, these tests, which had been scheduled for December 1990, were delayed until January 1991. The testing site was altered to allow the 53 ft span to be only one to two ft deep for safety in the event of bridge failure. The approximate locations and sizes of the typical cracks observed were shown in Figure 6.

7.1.2 Second Period - 23 Jan 91 to 12 Feb 91

Coupon crack growth was measured following numerous crossings. All eight coupon crack lengths were read. The bulge in coupon location 2 of Bridge A1-4 was more severe and it was repaired by removing the coupon, repeating surface preparation techniques, and remounting the coupon. The measured coupon crack lengths are presented in Table 7 with the loading histories calculated. The -10 coupon sets, designed for 10,000 crossings, do not have sufficient resolution for calculating this relatively small number of applied cycles. However, as can be

Table 6. Strain Gauge Data, Bridge A1-3, Coupon Set 1
53 ft Span, 8 Percent Incline, 70 Ton Vehicle

Crossing Number	Maximum Strain Cycle (uE)	
	Location 1 (2024-T3)	Location 2 (6061-T6)
1	2390	
2		2306
3	2197	
4		2132
5	2245	
6		2211
7	2382	
8		2305
9	2411	
10		2248
Average Strain Cycle = 2280 uE		

Table 7. Measured Crack Lengths as of 12 Feb 91

Bridge	Coupon Set Number	Attachment Location Number	Crack Tip-to-Tip Dec 90	Crack Tip-to-Tip 12 Feb 91	Calculated		Actual	
					Cycles	Stress	Cycles	Stress
A1-3	1	1	0.500	0.53	N/A	N/A		
		2	0.500	0.52				
	3	3	0.800	0.91	420	23.2	426	23.9
		4	0.900	1.00				
A1-4	2	1	0.500	0.53	N/A	N/A		
		2	0.500	0.53				
	4	3	0.800	0.91	420	23.2	406	23.9
		4	0.900	1.00				

clearly seen in the table, both of the -02 coupon sets showed sufficient growth and excellent representation of the actual loading history.

7.1.3 Third Period - 13 Feb 91 to 27 Feb 91

This visit was made to repair bulged coupons. During the course of the field tests, seven of the eight coupons, with the exception of Bridge A1-3, Set 3, Location 4, developed center bulges. All seven were removed and inspected. Water was found in all of the friction surfaces. However, it was not determined if water contamination was the cause of attachment slippage or the result of seal leakage from bulging. Blackening was also observed on the friction surfaces, as shown in Figure 24. This blackening indicates fretting due to relative movement during cycling.

Center bulging of a coupon occurs as a result of attachment slippage. Under high tension loading, the attachment friction may be insufficient, causing slippage and, consequently, reduced strain in the coupon. When the bridge is unloaded, the attachment friction is sufficient to prevent the coupon from slipping back to its original position. Thus, the coupon is loaded in compression and bulging results.

Five of the seven coupons removed were cleaned, resanded, degreased, and reapplied to their previous locations. Set 3 on Bridge A1-3 was replaced with new coupons as the coupons removed had been permanently deformed by the bulging. The new initial crack lengths were measured and are given in Table 8.

7.1.4 Fourth Period - 28 Feb 91 to 21 Mar 91

This visit was made to take final crack length readings from Bridge A1-3 which had completed the crossing tests. Set 3, the -02 coupon set on this bridge, was bulged and not functional. Set 1, the -10 coupon set on this bridge, was in good condition and crack length measurements were made. Calculations showed excellent agreement with the actual loading history as shown in Table 9.

The two coupon sets on bride A1-4 were bulged and thus not operational. Since these coupons were installed during the third visit, while the bridge was across a 53 ft span, the fact that the bridge was now placed directly on the ground and not under static load likely contributed to this bulging. However, the static load (~3 Ksi) is not sufficient to cause severe the bulging (~1/4 in.)

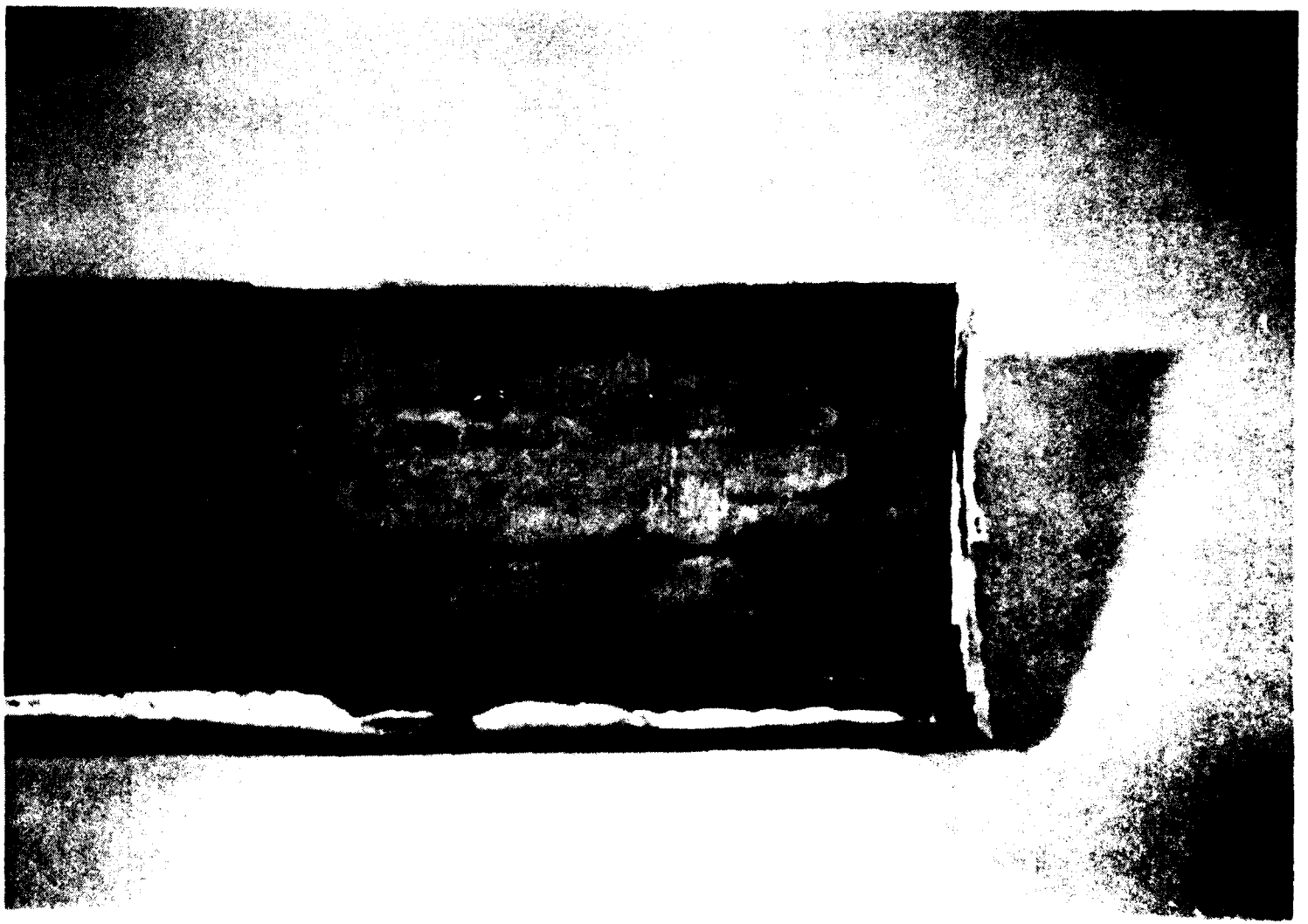

Figure 24. Typical Field Coupon Attachment Area

Table 8. Measured Crack Lengths as of 27 Feb 91

Bridge	Coupon Set Number	Attachment Location Number	Crack Tip-to-Tip 27 Feb 91	Comments
A1-3	1	1	0.56	
		2	0.58	
	3	3	0.81	New Coupon
		4	0.93	New Coupon
A1-4	2	1	0.53	
		2	0.54	
	4	3	1.02	
		4	1.12	

Table 9. Measured Crack Lengths as of 21 Mar 91

Bridge	Coupon Set Number	Attachment Location Number	Crack Tip-to-Tip 27 Feb 91	Crack Tip-to-Tip 21 Mar 91	Calculated		Actual	
					Cycles	Stress	Cycles	Stress
A1-3	1	1	0.56	0.60	720	19.1	740	18.1
		2	0.58	0.62				
	3	3	0.81	0.86	N/A	N/A		
		4	0.93	0.93				
A1-4	2	1	0.53	0.53	N/A	N/A		
		2	0.54	0.54				
	4	3	1.02	1.06	276	18.1	<20	N/A
		4	1.12	1.15				

Note: Set 4 crack growth likely due to bulging damage as negligible cycling occurred.

observed in Set 4. Therefore, it is likely that these coupons slipped during the few bridge crossing applied. It is important to note that the bulging (~0.08 in.) due to the static load of the bridge itself produces a stress in the coupon of only approximately 6 Ksi. However, a 1/4 in. bulge can produce a stress of more than 20 Ksi. As the crack growth observed in Set 4 was not the result of crossings, as is falsely indicated in Table 9, it was likely the result of the severe bulging. This set was permanently damaged and not repaired.

Set 2 on this bridge was not as severely bulged. This set was removed, cleaned, sanded, degreased, and reinstalled. Initial crack measurements were also shown in Table 9.

7.2 Static Test at Ft. Belvoir, VA

Both bridges were tested statically at Ft. Belvoir, VA following completion of the crossing tests. Bridge A1-3, from which both FLI coupon sets had already been removed, was successfully tested to 153 tons at a span of 53 ft. Foster-Miller personnel were on-site for the static test of Bridge A1-4 which had seen 800 crossings since the fourth visit to APG, MD. Coupon set 4 was severely bulged as it had been at APG. This set was removed and strain gauges were attached directly to the bridge at these two locations. Coupon set 2 was slightly bulged and left intact for strain measurements from the coupons during static testing.

Bridge A1-4 was statically tested to failure at 146 tons with a span of 53 ft. Failure occurred at a secondary hinge point, as indicated in Figure 25. Strain data were recorded on both the coupons and the bridge for this loading, presented in Figure 26. These data show that the strain is as expected - equivalent on both sides of the center hinge based on the data from the strain gauges attached directly to the bridge. The coupon strain gauges show an offset zero strain due to their bulging. However, they track along the same slope as the bridge gauges demonstrating nearly total strain transfer if the bulging offset is discounted.

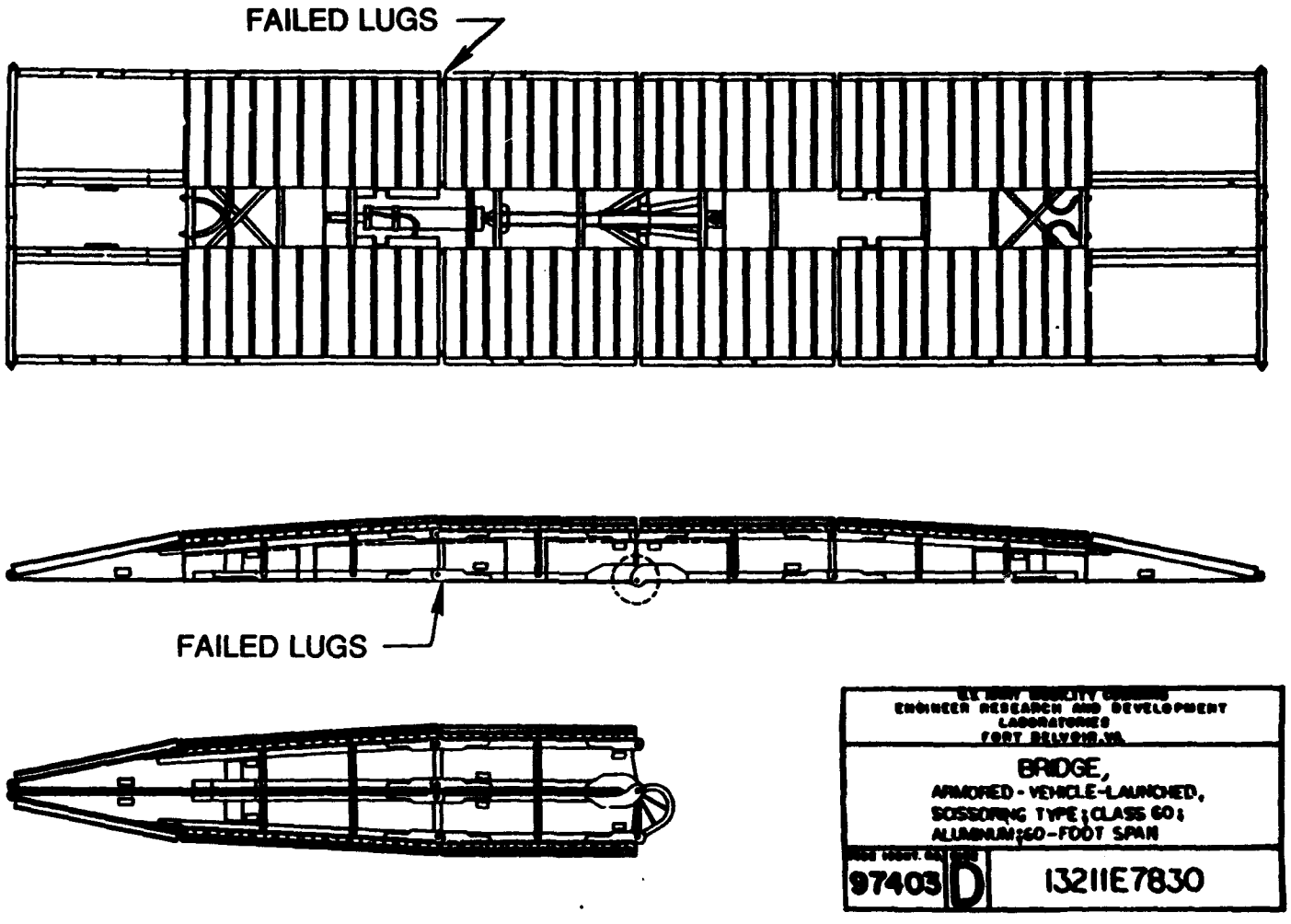

Figure 25. Failure of AVLB (A1-4)

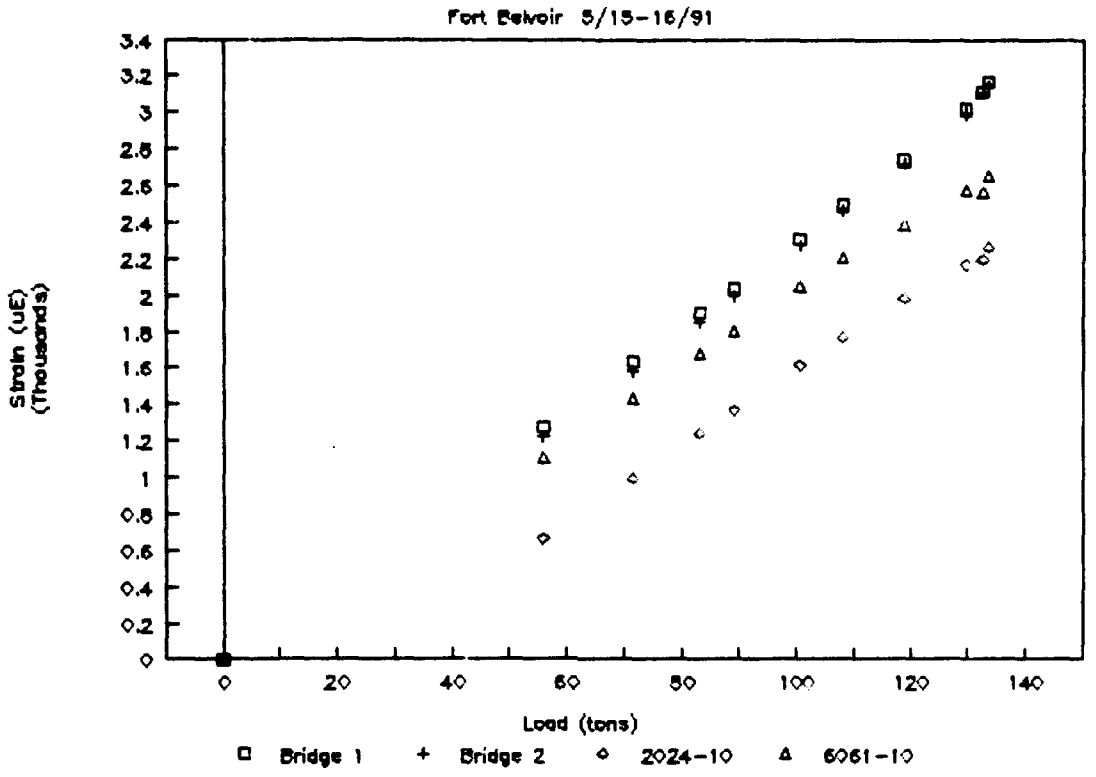

Figure 26. AVLB Static Load Test (A1-4), Ft. Belvoir May 15 to 16, 1991

8. OPTIMIZE COUPON SIZE

8.1 General Considerations

Several significant factors influenced coupon size reduction. The physical space available at the desired attachment location on the AVLB provided the upper bound for sizing. However, further size reduction was preferable to facilitate installation and adapt to alternate bridges.

The life of the indicating system was the primary design consideration for the free length of the coupon. Within this program, a target system life of 10,000 cycles at 20 Ksi was used. Therefore, the coupon size had to be sufficient to allow crack growth over this useful life without fully failing the coupon.

The final crack length after this cycling depends on the initial crack length. Smaller coupon sizing is attainable if smaller initial crack lengths can be used. Since the coupons can certainly be fabricated with smaller initial crack lengths, the minimum resolution of the crack measurement system became the primary driving factor in optimization of the free area size of the coupon.

In addition to the size of the free area of the coupon, the total size includes the attachment areas, which can influence the required size of the free area. With a bolted attachment, significant attachment area was required to meet the friction surface area requirements. A free length equal to at least twice the width of the coupon was also required to ensure a uniform stress field at the crack. The bonded attachment provided two size reduction advantages. The bonded area required was not as large at the required friction area and the stress field uniformity due to bonding greatly reduced the necessary free length.

8.2 Assembly D - Fully Bonded Coupon

Assembly D was tested under the same applied stress as Assembly C for comparative testing of the effects of reducing the coupon free length. The 6061-T6 coupon bonded area extended to within approximately 3/4 in. away from the crack. This left a coupon free length of 1.5 in. The 2024-T3 coupon was to have a similar free length. However, adhesive seepage inadvertently resulted in this coupon being fully bonded to the parent coupon with no free length.

The results from this test demonstrated an important factor in coupon size optimization. The 6061-T6 coupon crack growth was in good agreement with predicted crack growth for a stress of 16.2 Ksi, the average stress transfer demonstrated in Assembly C. The 2024-T3 coupon crack growth was substantially less than the predicted crack growth. This was likely due to a reduction in the stress intensity factor at the crack tip when the bond supports the material directly surrounding the crack tip. Figure 27 shows the crack growth for both coupons. Thus, while a fully bonded coupon was found to be unacceptable, a free length of only 1.5 in. was apparently acceptable.

8.3 Size Reduction Test

One test (Assembly E) was conducted to evaluate the potential for size reduction. For this assembly, a coupon size of 8 in. long by 3 in. wide was tested. The test assembly was similar to that of the previous full-scale tests with one FLI coupon bonded to either side of the parent coupon. The bonded areas extended approximately 3.75 in. on either end of the coupons. The center free length was approximately 0.5 in. Figure 28 shows this test assembly. Cycling was conducted at 20 Ksi and crack length measurements were made with the Krak Gage system.

The results from this test demonstrated that coupon width and free length will affect crack propagation. Figure 29 shows that stable crack growth was achieved to 70 percent of the width of the 6061-T6 coupon. However, the crack growth does not apparently follow the curve predicted by the Paris Law utilizing the constants defined for the 4 in. wide coupons. Additionally, the 2024-T3 coupon demonstrated retarded crack growth. This was likely due to adhesive seepage reduction of the free length. This test demonstrated that stable crack growth can be achieved in smaller coupons. However, further tests are required to fully characterize the finite width effects.

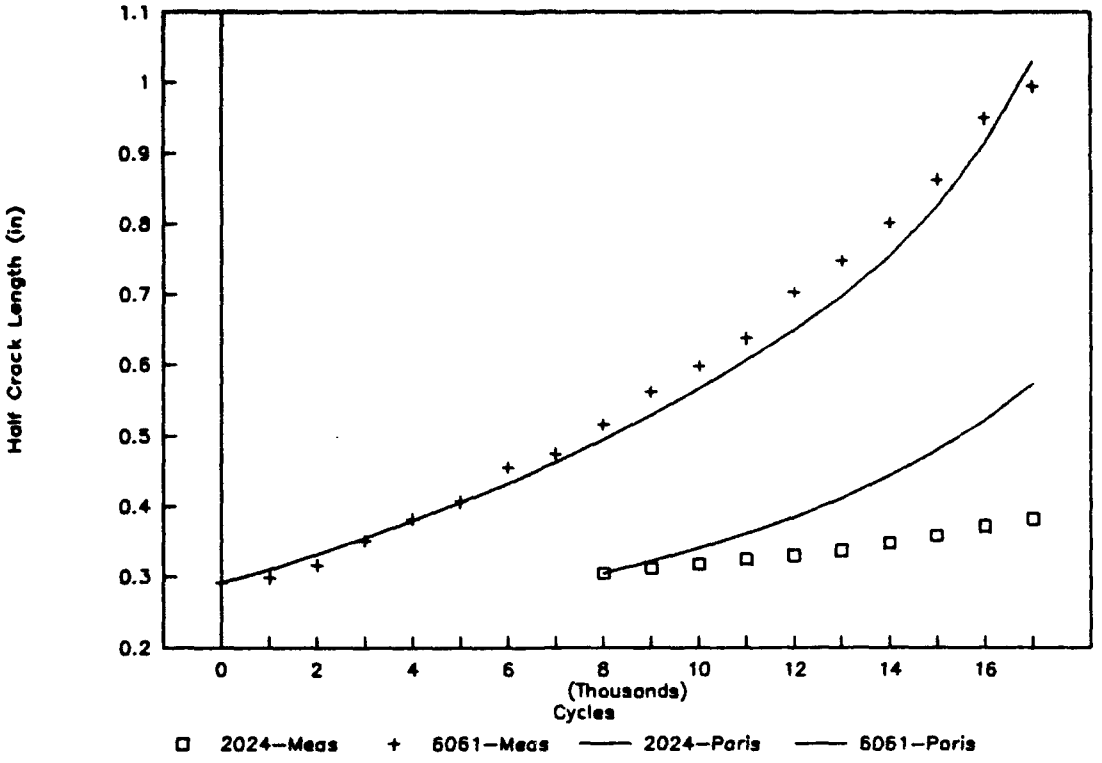

Figure 27. Assembly D, Crack Propogation (Measured versus Paris)

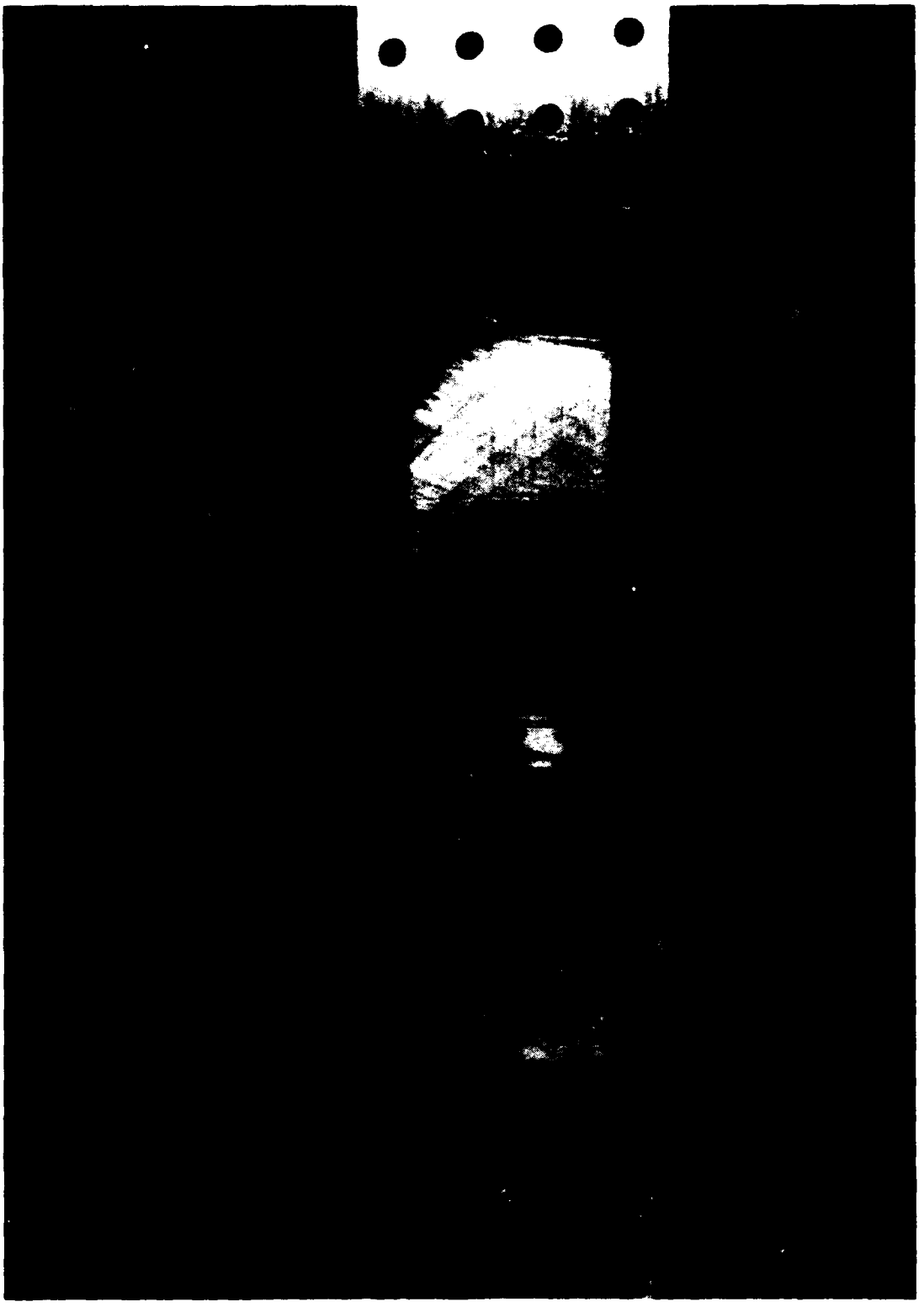

Figure 28. Coupon Optimization Test

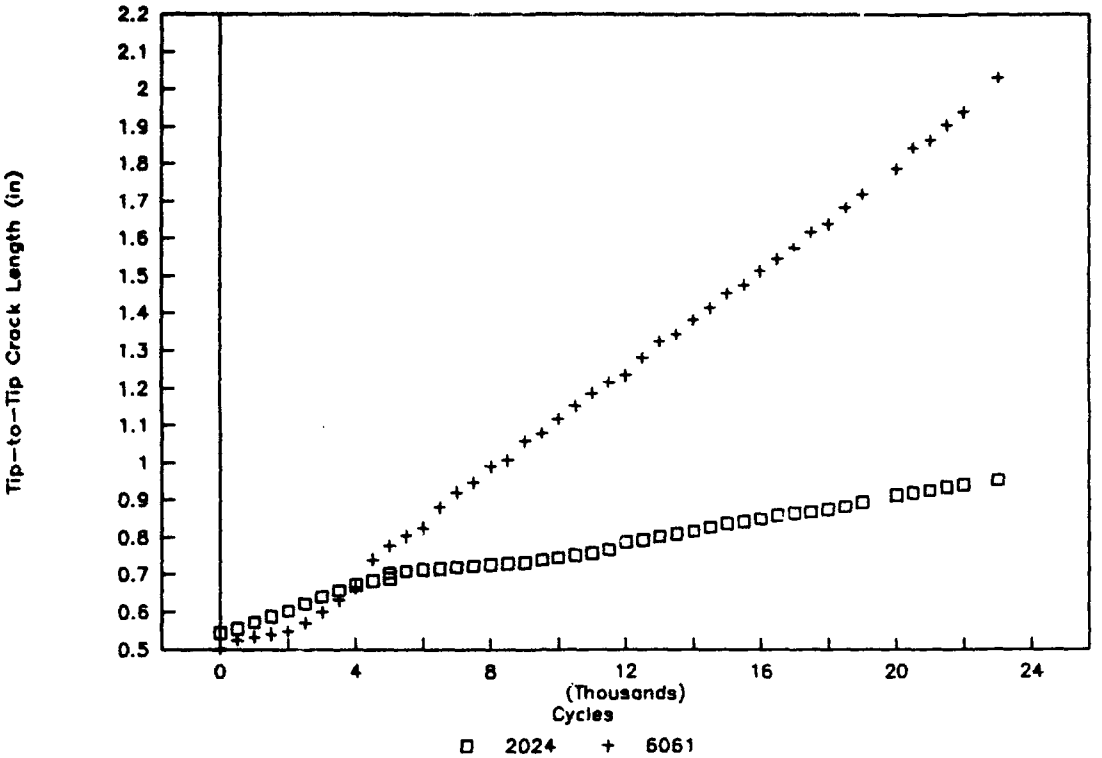

Figure 29. FLI Assembly E, Crack Propogation at 20 Ksi

9. CONCLUSIONS AND RECOMMENDATIONS

9.1 Conclusions

The Twin Coupon Fatigue Life Indicator system was successfully demonstrated in the vehicle crossing tests on the AVLB during the period of January to April 1991. A total of four, two-coupon sets were applied to the two AVLBs for 2000 crossing tests at Aberdeen Proving Grounds. The test results provided adequate proof of the Twin Coupon concept.

The bridge crossing histories were accurately resolved from the crack length data recorded at these tests. Typical predicted results were within 5 percent of the measured stresses. The calculated number of cycles was typically within 5 percent of actual.

Bonded assembly laboratory tests also demonstrated that the stress histogram can be accurately resolved from the two crack lengths. The data from Assemblies B and C indicated numbers of cycles and stress levels within 10 percent of actual. The latter took into account the 20 percent reduction in strain transfer consistently observed in the bonded attachment.

The computer software to resolve the loading history from the coupon crack lengths, developed previously on the basis of laboratory test data, can be reliably applied for field conditions. However, for analysis of the -02 coupons, only the upper line of the bi-linear 6061-T6 fit is used and no iteration is done.

The error due to the manual measurement of crack length using a microscope in the field tests was about 0.01 in. Laboratory tests showed that remote crack length measurement can be accomplished automatically with either the Krak Gage system or the ladder gauges. The Krak Gage system, which demonstrated an error of less than +/- 0.001 in., was significantly superior in all performance aspects and can be expected to perform well in the field.

AVLB crossing tests with bolted coupon attachments yielded good results validating the Twin Coupon concept. However, coupon slippage occurred and the bolted attachment needed repairs and readjustments.

The bonded attachment was successfully demonstrated in the laboratory and can be expected to be the preferable attachment method for field usage. The Tra-Bond 2143D epoxy and Devcon

Aluminum Putty demonstrated acceptable performance for this application. The Martin Marietta Laboratories epoxy performed well with strict adherence to the surface preparation requirements. These requirements can be met in the field and this epoxy may be preferable in an adverse environment.

Significant coupon size reduction potential was demonstrated in the laboratory. This was possible due to the success of the bonded attachment method and the improved resolution of a remote crack measurement system.

9.2 Recommendations

Further testing will be required to validate the performance of the optimized coupon size presented in this report. These tests will also be necessary to determine the coupon geometry effects on stress intensity factor (SIF) associated with the reduced size. These tests should also investigate the effects of compression loading which will occur during launching of the bridge.

Field tests with the bonded attachment method will be valuable to further validate the Twin Coupon FLI system under actual crossing loads. These tests would demonstrate the system as a practical tool for the Army.

Sealing of the coupons was done with a silicone sealant during the field proof-of-concept tests. However, due to the difficulty in sealing a "bolted attachment" and the need to break the seal for optical crack measurement, some rain water seepage occurred. A similar sealing method, with bonded coupons and a remote crack measurement system, will work efficiently, but this needs to be demonstrated by field environment tests.

Additional testing needs to be conducted to further develop the Twin Coupon FLI for broader application to all types of bridges. The optimized size and the bonded attachment method provide the potential for adaptation to alternate structures of various cross sections such as circular tubes.

Further analysis of the test data should be conducted to determine if computer software improvements can be made to eliminate the need for a bi-linear fit of the 6061-T6 data. This would eliminate the need for an iterative program.

APPENDIX A
FULL-SCALE TEST RESULTS

Assembly B

	2024-T3		6061-T6 (Right Side Only)			
Cycles	KrakGage (in)	Measured (in)	KrakGage (in)	Measured (in)	2a Measured (in)	Comments
0		0.56			0.50	Measured
4000	0.592					
5742	0.652		0.064	0.08		
9500	0.764	0.81				
10800	0.815					
12500	0.915	0.92	0.264	0.29	0.98	Proportioned
14000	0.956	0.97				
15300	1.063	1.06	0.607	0.57	1.66	Proportioned
16700		1.15		0.70	1.97	Measured

Note: The Krak Gage on the left half of the crack on the 6061-T6 Coupon did not function due to improper application. Optical measurements were made only on the right half for comparison to the Krak Gage output. The entire crack length was scaled from the right side measurement as follows:

Final tip to tip crack length = 1.97
Crack length between left and right Krak Gage = 0.28

Final crack length in gages = 1.69

Final measured crack length in right half = 0.70

Right half proportion of total = 0.70/1.69 = 0.414

Thus:

$2a = (a/0.414) + 0.28$

@12500 Cycles

$2a = (0.29/0.414) + 0.28 = 0.98$

@15300 Cycles

$2a = (0.57/0.414) + 0.28 = 1.66$

Full-Scale Bonded Assembly

Assembly C

Cycles	2024-T3 KrakGage (in.)	2024-T3 Measured (in.)	6061-T6 KrakGage (in)	6061-T6 Measured (in)
0	0.682		0.600	
1000	0.716		0.620	
2000	0.777	0.84	0.642	0.70
3300	0.836		0.687	
4000	0.885	0.93	0.714	
5000	0.951			
6000	1.027	1.04	0.801	
7000	1.106	1.15	0.862	0.89
8600	1.282	1.30	0.937	
10000	1.497	1.40	1.023	1.05
11000	1.607	1.55	1.085	1.10
12000	1.784	1.75	1.137	1.15
13000			1.199	1.20
14000	2.143	2.10	1.258	1.25
15000	2.328	2.30	1.308	1.35
16000	2.518	2.50	1.378	1.40
17000	2.793	2.70	1.445	1.45
18000	3.174		1.499	1.50
19000			1.566	1.55
20000			1.597	
21000			1.702	1.72
22300			1.813	1.80
23000			1.861	1.86
24000			1.968	1.96
25000			2.010	2.00
26000			2.098	
26500			2.146	

Full-Scale Bonded Assembly
(2024-T3 coupon bonded over entire length)

Assembly D

	Krak Gage Readings (mm)				2a (in)	
Cycles	1	2	3	4	2024	6061
0	0.08	0.06	0.06	0.05	0.586	0.584
1000	0.09	0.06	0.24	0.19	0.586	0.597
2000	0.08	0.06	0.73	0.63	0.586	0.634
3000	0.08	0.06	1.58	1.51	0.586	0.702
4000	0.08	0.06	2.41	2.24	0.586	0.763
5000	0.08	0.06	3.09	2.84	0.586	0.813
6000	0.09	0.11	4.17	4.21	0.588	0.910
7000	0.16	0.25	4.89	4.47	0.596	0.949
8000	0.33	0.42	5.56	5.90	0.610	1.031
9000	0.51	0.58	7.17	6.62	0.623	1.123
10000	0.59	0.82	8.04	7.60	0.636	1.196
11000	0.70	1.07	9.17	8.49	0.650	1.275
12000	0.79	1.25	10.62	10.37	0.660	1.406
13000	0.93	1.46	11.72	11.56	0.674	1.497
14000	1.19	1.73	12.84	13.14	0.695	1.603
15000	1.40	2.04	14.13	14.94	0.715	1.724
16000	1.87	2.31	15.65	17.87	0.745	1.900
17000	2.14	2.54	17.48	18.32	0.764	1.989
18000	2.41	2.83	19.16	18.87	0.786	2.077
19000	2.65	3.16	20.70	21.12	0.809	2.226
20000	2.88	3.49	22.49	23.47	0.831	2.389
21000	3.16	3.82	24.19	25.23	0.855	2.526

Reduced Size Bonded Assembly

Assembly E

	Krak Gage Readings (mm)				2a (in)	
Cycles	1	2	3	4	2024	6061
0	0.035	0.074	0.131	0.141	0.544	0.501
500	0.055	0.329	0.389	0.166	0.555	0.524
1000	0.188	0.635	0.621	0.259	0.572	0.533
1500	0.332	0.883	0.935	0.350	0.588	0.541
2000	0.467	1.126	0.999	0.474	0.603	0.546
2500	0.684	1.390	1.325	0.729	0.622	0.571
3000	0.923	1.637	1.629	1.150	0.641	0.599
3500	1.145	1.841	2.005	1.595	0.658	0.632
4000	1.307	2.061	2.323	2.109	0.673	0.664
4500	1.460	2.181	3.846	2.503	0.683	0.740
5000	1.533	2.233	4.417	2.691	0.688	0.778
5000	1.509	2.655	4.396	2.900	0.704	0.777
5500	1.605	2.712	4.713	3.256	0.710	0.804
6000	1.650	2.754	5.953	3.562	0.713	0.825
6500	1.691	2.783	5.925	4.711	0.716	0.881
7000	1.754	2.821	6.567	4.393	0.721	0.921
7500	1.798	2.854	6.830	4.727	0.723	0.947
8000	1.854	2.887	7.586	5.112	0.727	0.990
8500	1.897	2.922	7.758	5.362	0.730	1.007
9000	1.932	2.967	8.489	5.946	0.733	1.058
9500	1.996	3.065	8.650	6.297	0.739	1.078
10000	2.067	3.154	9.258	6.655	0.746	1.116
10500	2.184	3.211	9.553	7.263	0.752	1.152
11000	2.250	3.262	10.149	7.548	0.757	1.187
11500	2.402	3.347	10.389	8.030	0.766	1.215
12000	2.526	3.763	10.510	8.378	0.782	1.237
12500	2.596	3.921	11.389	8.726	0.793	1.281
13000	2.676	3.993	12.036	9.169	0.803	1.325
13500	2.745	4.067	12.237	9.469	0.806	1.345
14000	2.876	4.131	12.560	10.103	0.816	1.383
14500	2.991	4.302	13.115	10.368	0.827	1.415
15000	3.090	4.437	13.619	10.804	0.836	1.452
15500	3.172	4.475	14.027	11.015	0.841	1.475
16000	3.304	4.555	14.284	11.390	0.849	1.512
16500	3.451	4.635	14.769	12.042	0.858	1.546
17000	3.524	4.695	15.225	12.310	0.864	1.574
17500	3.554	4.773	15.755	12.852	0.868	1.616
18000	3.667	4.835	16.057	13.104	0.875	1.638
18500	3.756	4.934	16.491	13.602	0.882	1.683
19000	3.855	5.108	17.078	14.111	0.893	1.718
19500		5.239		14.655		
20000	4.139	5.348	18.079	14.851	0.914	1.786
20500	4.218	5.415	18.755	15.567	0.919	1.841
21000	4.315	5.491	19.191	15.671	0.926	1.863
21500	4.416	5.599	19.637	16.276	0.934	1.904
22000	4.482	5.699	Measured		0.941	1.94
23000	4.617	5.863	Measured		0.953	2.03